Heliyon 10 (2024) e27916

Contents lists available at ScienceDirect

Heliyon

journal homepage: www.cell.com/heliyon

Research article

# The predictive model of hydrobiological diversity in the Asana-Tumilaca basin, Peru based on water physicochemical parameters and sediment metal content

Lisveth Flores del Pino [a], Nancy Marisol Carrasco Apaza [a], Víctor Caro Sánchez Benites [a], Lena Asunción Téllez Monzón [a], Kimberly Karime Visitación Bustamante [a], Jerry Arana-Maestre [b], Diego Suárez Ramos [a], Ayling Wetzell Canales-Springett [a], Jacqueline Jannet Dioses Morales [a], Evilson Jaco Rivera [c], Alex Uriarte Ortiz [d], Paola Jorge-Montalvo [a,*], Lizardo Visitación-Figueroa [a]

[a] *Center for Research in Chemistry, Toxicology, and Environmental Biotechnology, Department of Chemistry, Faculty of Science, Universidad Nacional Agraria La Molina, 15024, Lima, Peru*
[b] *Museum of Natural History, Department of Limnology, Universidad Nacional Mayor de San Marcos, 15072, Lima, Peru*
[c] *Universidad Politécnica de Cataluña, 08034, Barcelona, Spain*
[d] *Organismo de Evaluación y Fiscalización Ambiental (OEFA), Ministerio Del Ambiente, 15076, Lima, Peru*

ARTICLE INFO

*Keywords:*
Glacial melt
Hydrochemistry
Taylor diagram
Volcanic soils
Weathering

ABSTRACT

The hydrobiological diversity in the basin depends on biotic and abiotic factors. A predictive model of hydrobiological diversity for periphyton and macrobenthos was developed through multiple linear regression analysis (MLRA) based on the physicochemical parameters of water (PPW) and metal content in sediments (MCS) from eight monitoring stations in the Asana-Tumilaca Basin during the dry and wet seasons. The electrical conductivity presented values between 47.9 and 3617 μS/cm, showing the highest value in the Capillune River due to the influence of geothermal waters. According to Piper's diagram, the water in the basin had a composition of calcium sulfate and calcium bicarbonate-sulfate. According to the Wilcox diagram, the water was found to be between good and very good quality, except for in the Capillune River. The Shannon–Wiener diversity indices (H′) were 2.62 and 2.88 for periphyton, and 2.10 and 2.44 for macrobenthos, indicating moderate diversity; for the Pielou's evenness index (J′), they were 0.68 and 0.70 for periphyton, and 0.68 and 0.59 for macrobenthos, indicating similar equity, in the dry and wet seasons, respectively, for both indices. In the model there were three cases, where the first two cases only worked with PPW or MCS, and case 3 worked with PPW and MCS. For case 3, the predicted values for H′ and J′ of periphyton and macrobenthos concerning those observed presented correlation coefficients of 0.7437 and 0.6523 for periphyton and 0.9321 and 0.8570 for macrobenthos, respectively, which were better than those of cases 1 and 2. In addition, principal component analysis revealed that the As, Pb, and Zn contents in the sediments negatively influenced the diversity, uniformity, and richness of the macrobenthos. In contrast, Cu and Cr had positive impacts because of the adaptation processes.

* Corresponding author.
*E-mail address:* paolajom@lamolina.edu.pe (P. Jorge-Montalvo).

https://doi.org/10.1016/j.heliyon.2024.e27916
Received 29 November 2023; Received in revised form 26 February 2024; Accepted 8 March 2024
Available online 14 March 2024

**Abbreviations**

| | |
|---|---|
| As | Arsenic in sediment |
| Hg | Mercury in sediment |
| Cd | Cadmium in sediment |
| Cu | Copper in sediment |
| Cr | Chromium in sediment |
| Pb | Lead in sediment |
| Zn | Zinc in sediment |
| H' | Shannon-Wiener index |
| J' | Pielou's evenness index |
| EC | Electrical conductivity |
| DO | Dissolved oxygen |
| pH | Hydrogen potential |
| T | Temperature |
| $HCO_3^-$ | Bicarbonates |
| Cl | Chlorides |
| $SO_4^2$ | Sulfates |
| Ca | Total calcium |
| Mg | Total magnesium |
| K | Total potassium |
| Na | Total sodium |
| RAS | Sodium absorption ratio |
| ISQG | Interim Sediment Quality Guideline |
| PEL | Probable Effect Level |
| INGEMMET | Geological, Mining and Metallurgical Institute |
| NDSI | Normalized Difference Snow Index |
| MLRA | Multiple linear regression analysis |
| RMSE | Root mean square error |
| PCA | Principal component analysis |
| PPW | Physicochemical parameters of water |
| MCS | Metal content in sediments |
| DS | Dry season |
| WS | Wet season |

## 1. Introduction

The diversity of aquatic life within a river basin is determined by several factors, such as physicochemical parameters of water (PPW), metal content in sediments (MCS), flow variations, and regional climate conditions [1,2]. The PPW are determined by the concentration of dominant cations and anions, which are in turn influenced by factors such as precipitation, weathering, and evaporation [3]. To preserve aquatic diversity, it is crucial to distinguish between natural and anthropogenic sources and understand the elements that can modify water chemistry. This understanding also encompasses the movement of pollutants and the composition of groundwater [4].

Physicochemical parameters, including dissolved oxygen (DO), biochemical oxygen demand (BOD), chemical oxygen demand (COD), pH, temperature, electrical conductivity (EC), bicarbonates, chlorides, sulfates, calcium, magnesium, potassium, and sodium are used to assess water quality [5,6]. The values of these parameters are represented by Piper and Wilcox diagrams, which indicate the type of water used according to the abundance of dominant ions and the quality of water used for irrigation, respectively [7,8].

Heavy metals present in sediments are ecologically significant because of their toxicity and tendency to accumulate in organisms. These nonbiodegradable heavy metals are integrated into the global ecological cycle and pose cumulative and toxic threats to aquatic ecosystem organisms [9,10]. Previous studies have demonstrated accumulation of heavy metals in plankton, benthos, fish, and humans. To evaluate the toxicity of sediment metals on aquatic organisms, the Canadian Sediment Quality Guidelines for the protection of aquatic life incorporate the Interim Sediment Quality Guideline (ISQG), the interim sediment quality reference value, and the Probable Effect Level (PEL) [1]. Sediments exceeding ISQG and PEL values may potentially harm aquatic organisms, although these values alone do not provide a complete prediction of the frequency, nature, and severity of biological effects [11].

Previous research in the upper Asana-Tumilaca Basin in the southern Peruvian Andes found that the hydrochemistry of the water is of a calcium sulfate nature, mainly influenced by the weathering process of the rock [8]. This is closely related to the presence of volcanic soils in the region and the melting of glaciers, which results in the exposure of new, easily erodible soils owing to the steepness of the terrain [8,12]. Glacier melting affects the quantity and quality of water, which subsequently affects biotic components. This is due to the emergence of new, erosion-prone soils that are often rich in aluminum and other minerals. The extent of glacial melt zones

can be assessed using the Normalized Difference Snow Index (NDSI). The NDSI quantifies the relative difference in reflectance between ultraviolet (UV) and infrared light, allowing snow to be distinguished from other surfaces [13].

In hydrobiological monitoring in river basins, hydrobiological indices, such as the Shannon–Wiener diversity index and Pielou's evenness, are used to determine the diversity of hydrobiological communities, such as periphyton and macrobenthos (benthic macroinvertebrates) [14,15]. Periphyton are widely distributed organisms with a high colonization rate, which makes them particularly sensitive to external disturbances such as increased flow and the presence of suspended materials that can have an abrasive effect, reducing light penetration into the riverbed [2]. Macrobenthos, a group of commonly used biological indicators, are valuable tools for assessing the quality of surface water resources and aquatic ecosystems [16]. Relationships exist among the hydrobiological indices, macrobenthos composition patterns, and various environmental factors. These factors include increased flow, current velocity, alterations in benthic macroinvertebrate community structure, drift of many benthic macroinvertebrates, changes in habitat structure and ecological functions [17–19]. The assessment of hydrobiological diversity contributes to advancing ecological theory and helps in making informed decisions and recommendations for river basin management and conservation.

Predictive models are useful tools for risk management because they are reliable, accurate, and provide data on eminent risks [5,20]. Few studies have modeled hydrobiological diversity indices based on water physicochemical parameters [21,22], although these models can be improved by including other parameters such as MCS.

The objective of the present study was to develop a predictive model of hydrobiological diversity for periphyton and macrobenthos in the Asana-Tumilaca Basin using multiple linear regression analysis (MLRA) and to represent the results using a Taylor diagram. This study was conducted at eight monitoring stations in the basin during the dry and wet seasons. Water physicochemical parameters such as EC, DO, pH, temperature, and concentrations of bicarbonate, chloride, sulfate, sodium, potassium, calcium, and magnesium were analyzed and are represented in Piper and Wilcox diagrams. The concentrations of metals such as arsenic, mercury, cadmium, copper, chromium, lead, and zinc in the sediments were compared using the ISQG and PEL indices. Species richness was analyzed, and Shannon–Wiener diversity and Pielou's evenness indices were calculated and compared with data predicted by models based on PPW and MCS. Principal component analysis (PCA) was used to investigate the relationships between these variables. In addition, the NDSI was used to assess the degree of melting of the Arundane and Chuquiananta glaciers.

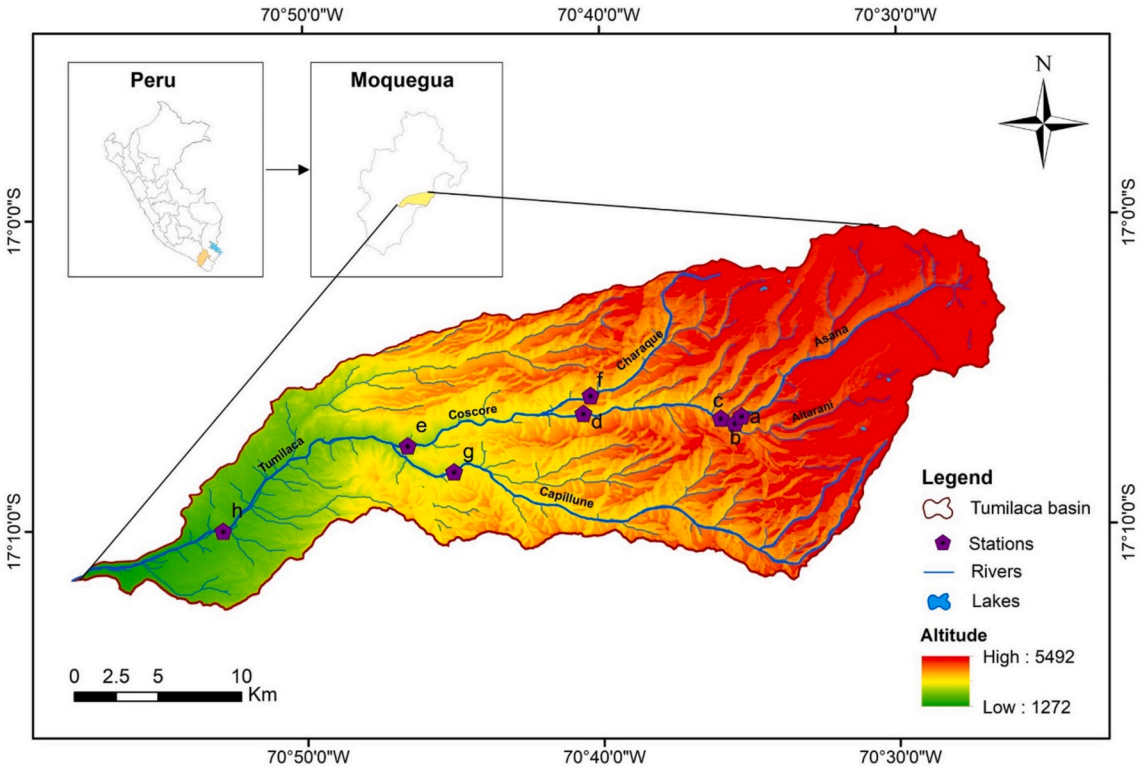


**Fig. 1.** Monitoring stations along the Asana-Tumilaca River Basin: Asana 1 (a), Altarani (b), Asana 2 (c), Asana 3 (d), Asana 4 (e), Charaque (f), Capillune (g), and Tumilaca (h).

## 2. Methodology

### 2.1. Study area

The study area encompasses eight monitoring stations situated along the Asana (Asana 1, Asana 2, Asana 3, Asana 4), Altarani, Capillune, Charaque, and Tumilaca rivers in the Asana-Tumilaca Basin, located in Moquegua, Peru, within the Western Andes (Fig. 1a–h). This area is mainly influenced by the deglaciation of snow-capped mountains as a result of climate change, soil mass movement, and rock erosion processes [8], which, in turn, influence the hydrobiological diversity of the basin. The initial conditions of the basin make it possible to evaluate biological diversity during mining activities that will occur in this area. In this region, investigations have been conducted to analyze the PPW, MCS, glacial coverage, and hydrobiological diversity. The Asana River originates from the volcanic glaciers of Arundani and Chuquiananta [8], an area subject to continuous glacial melting and the erosion of exposed soils. These rivers traverse ecological zones classified as tundra, humid forest, desert shrubland, and arid desert. The Asana-Tumilaca Basin spans an elevation range of 5492-1912 m above sea level (masl) and experiences a temperate sub-humid and cold boreal climate. Seasonal annual precipitation varies from 243 to 460 mm per year, primarily from January to March [23], with the dry season extending from May to December. The primary use of water in the basin is for irrigation, with secondary applications including human consumption, industrial use, and mining.

### 2.2. Evaluation of the PPW and MCS

The results of six water and sediment quality assessments were analyzed, with three conducted during the dry season (2013, 2017, and 2020) and three during the wet season (2014, 2018, and 2019). These assessments were part of a participatory environmental monitoring program for establishing an environmental baseline for a mining project in the region (data from 2013 to 2014 and 2017) and the surveillance monitoring program conducted by the Peruvian Agency for Environmental Assessment and Enforcement (data from 2018 to 2020).

To assess the PPW, on-site measurements of EC, DO, pH, and temperature were conducted. The bicarbonate content was assessed using the volumetric method outlined in SMEWW-APHA-AWWA-WEF 2320B, whereas the chloride and sulfate contents were determined using anion chromatography, as described in EPA METHOD 300.1. Additionally, sodium, calcium, magnesium, and potassium concentrations were measured as total metals using an ICP-MS instrument following EPA method 6020A. The main mechanisms governing the nature of water bodies in this area are rock weathering and the entry of geothermal water that influences the composition of the ions, EC, temperature, and DO [8]. However, in areas with low populations, concentrations of organic matter

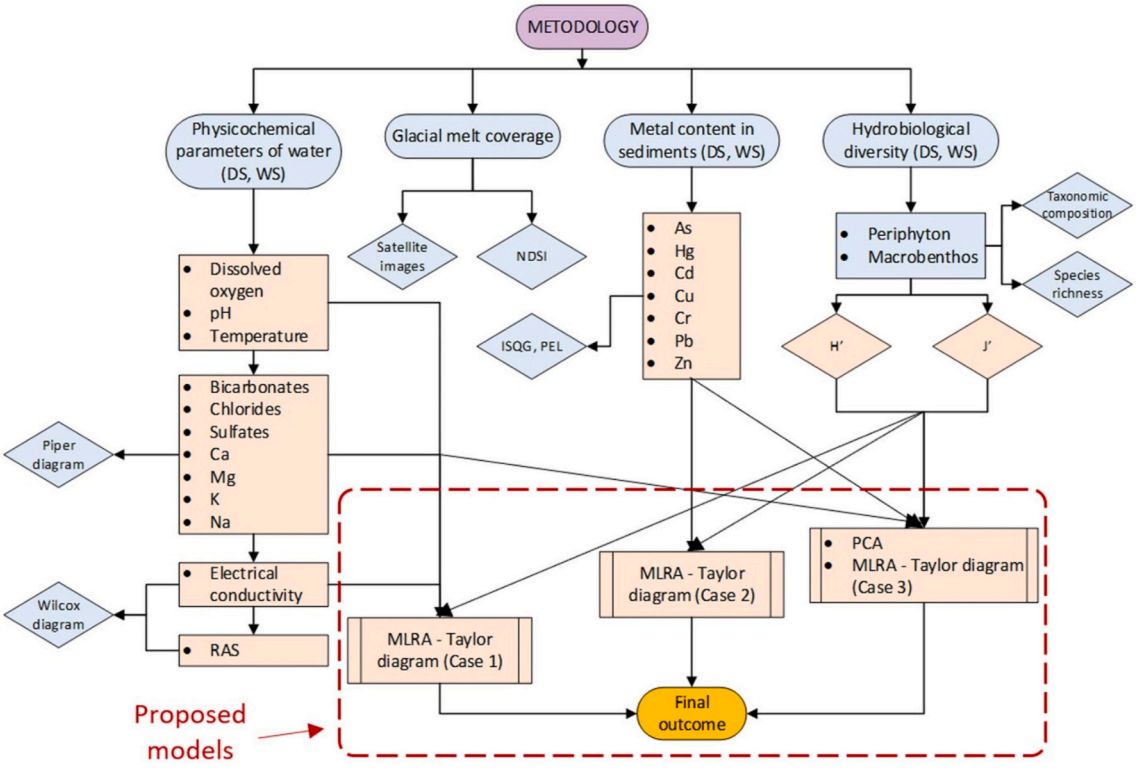


**Fig. 2.** Flow chart for methodology and proposed models.

expressed as BOD and COD were not detected, nor was the presence of thermotolerant coliforms detected. The results for anions and cations were plotted on a Piper diagram to determine the water classification in the basin. The Wilcox index was also determined as a function of the sodium adsorption ratio and EC to determine the water quality for agricultural use [7].

To evaluate the MCS, heavy metal concentrations were determined using ICP-MS equipment, following the guidelines outlined in EPA method 200.8. The metals evaluated were As, Hg, Cd, Cu, Cr, Pb, and Zn. The results were compared with the ISQG, interim sediment quality value, and PEL.

### 2.3. Glacier melt coverage assessment

Satellite images and the NDSI were used to track how the melting area changed over time and its influence on the study area. This comparison involved analyzing images from the dry seasons of 2013 and 2017 and those from the wet seasons of 2014 and 2018, and comparing the wet season of 2019 with the dry season of 2020. Areas covered by snow or ice were considered potential indicators of regions at risk of soil erosion caused by glacial melting.

### 2.4. Evaluation of the hydrobiological community

The results of six hydrobiological monitoring assessments were examined, which included analyzing periphyton and macrobenthos using the SMEWW-APHA-AWWA-WEF Part 10 300 C and 500 C methods (22 nd Ed, 2012), respectively. Diversity was assessed using the Shannon-Wiener index, classifying values below 1.5 as low diversity, values between 1.5 and 3.5 as moderate diversity, and values between 3.5 and 5 as high diversity [24,25]. Species richness was estimated as the total number of different species found at a monitoring station, and the Pielou's evenness index was calculated to measure the proportion of the observed diversity relative to the maximum expected diversity. This index ranges from zero to one, where one corresponds to a situation in which all species are equally abundant [15].

A predictive model for hydrobiological diversity indices was proposed by evaluating three cases: case 1 used PPW data, case 2 used MCS data, and case 3 used PPW and MCS data (Fig. 2). MLRA was used for each case, and the results were represented by a Taylor plot as a function of the normalized standard deviation, correlation coefficient (R), and root mean square error (RMSE) [20]. The assumptions of the model were checked by assessing the normality of the residuals using the Shapiro–Wilk test and the homogeneity of variances.

### 2.5. Statistical analysis

The minimum, maximum, and mean values of the PPW and MCS of the rivers of the Asana-Tumilaca Basin are reported in Tables 1–3. Conversely, all basin monitoring data (PPW, MCS, and, hydrobiological diversity indices) were represented by box plots, and their distributions was analyzed using the Jarque–Bera test. PCA was used to assess the spatiotemporal variability of hydrobiological diversity in the Asana-Tumilaca Basin and its relationship with PPW and MCS. PCA is one of the most widely accepted

**Table 1**
Mean findings of the physicochemical water parameters at monitoring stations in the Asana-Tumilaca Basin during the dry (2013, 2017, and 2020) and wet (2014, 2018, and 2019) seasons.

| Monitoring stations | | Electrical conductivity | | Dissolved oxygen | | | | pH | | | Temperature | | |
|---|---|---|---|---|---|---|---|---|---|---|---|---|---|
| | | μS/cm | | mg/L | | | | | | | %C | | |
| | | Min | Max | Mean | Min | Max | Mean | Min | Max | Mean | Min | Max | Mean |
| Asana 1 | DS | 115.8 | 170.8 | 143.3 | 5.9 | 7.3 | 6.6 | 7.5 | 7.7 | 7.6 | 9.2 | 15.2 | 12.2 |
| | WS | 144.1 | 154.5 | 149.3 | 7.5 | 7.9 | 7.7 | 7.6 | 7.8 | 7.7 | 6.9 | 13.1 | 10 |
| Altarani | DS | 47.9 | 162.9 | 105.4 | 5.9 | 7.1 | 6.5 | 7.2 | 8 | 7.6 | 10.9 | 14.9 | 12.9 |
| | WS | 49.4 | 70.8 | 60.1 | 6.8 | 7 | 6.9 | 7.8 | 8.2 | 8 | 9.9 | 14.9 | 12.4 |
| Asana 2 | DS | 114.6 | 135 | 124.8 | 6.3 | 7.1 | 6.7 | 7.4 | 7.8 | 7.6 | 11.2 | 13 | 12.1 |
| | WS | 111.4 | 138.2 | 124.8 | 6.8 | 7.4 | 7.1 | 7.4 | 8.2 | 7.8 | 9.7 | 14.7 | 12.2 |
| Asana 3 | DS | 148.3 | 163.1 | 155.7 | 6.2 | 7.2 | 6.7 | 6.8 | 7.8 | 7.3 | 13.2 | 15.2 | 14.2 |
| | WS | 140.6 | 180.6 | 160.6 | 7.4 | 7.6 | 7.5 | 6.4 | 7.8 | 7.1 | 10.4 | 14.4 | 12.4 |
| Asana 4 | DS | 151.3 | 170.3 | 160.8 | 5.5 | 7.5 | 6.5 | 7.4 | 7.8 | 7.6 | 12 | 17.2 | 14.6 |
| | WS | 136.7 | 173.3 | 155 | 7.5 | 8.5 | 8 | 7.1 | 7.5 | 7.3 | 10 | 10.6 | 10.3 |
| Charaque | DS | 79.9 | 100.1 | 90 | 5.6 | 7.2 | 6.4 | 7.5 | 7.7 | 7.6 | 12.1 | 15.1 | 13.6 |
| | WS | 81.9 | 104.7 | 93.3 | 6.7 | 7.3 | 7 | 7.9 | 8.1 | 8 | 12.2 | 17.2 | 14.7 |
| Capillune | DS | 801.6 | 2348.6 | 1575 | 6 | 7.6 | 6.8 | 8.2 | 8.4 | 8.3 | 16.7 | 20.5 | 18.6 |
| | WS | 1275.9 | 3616.7 | 2446 | 5.5 | 7.7 | 6.6 | 8.1 | 8.7 | 8.4 | 14.1 | 22.7 | 18.4 |
| Tumilaca | DS | 202.6 | 339 | 270.8 | 6.1 | 9.7 | 7.9 | 7.5 | 8.1 | 7.8 | 12.7 | 18.5 | 15.6 |
| | WS | 342.7 | 370.7 | 356.7 | 8.1 | 8.3 | 8.2 | 8.1 | 8.5 | 8.3 | 15.8 | 18.8 | 17.3 |
| WQS Cat 4 River OMS Global average* | | 1000 | | | 5 | | | 6.5–9 | | | | | |

DS: dry season April–December, WS: wet season January–March. *
Source: Tsering et al. [30].

**Table 2**
Mean findings of the major water ions at monitoring stations in the Asana-Tumilaca Basin during the dry (2013, 2017, and 2020) and wet (2014, 2018, and 2019) seasons.

| Monitoring stations | | Bicarbonates | | | Chlorides | | | Sulfates | | | Ca | | | Mg | | | K | | | Na | | |
|---|---|---|---|---|---|---|---|---|---|---|---|---|---|---|---|---|---|---|---|---|---|---|
| | | mg/L | | | | | | | | | | | | | | | | | | | | |
| | | Min | Max | Mean | Min | Max | Mean | Min | Max | Mean | Min | Max | Mean | Min | Max | Mean | Min | Max | Mean | Min | Max | Mean |
| Asana 1 | DS | 16.5 | 24.9 | 20.7 | 0.6 | 1.2 | 0.9 | 31.2 | 52.4 | 41.8 | 10 | 21.7 | 16 | 2.2 | 5 | 3.6 | 1.3 | 2.5 | 1.9 | 5 | 11.6 | 8.3 |
| | WS | 17.2 | 25.4 | 21.3 | 0.6 | 1.4 | 1 | 41.3 | 48.3 | 44.8 | 14 | 16.3 | 15.1 | 2.8 | 3.6 | 3.2 | 1.9 | 2.5 | 2.2 | 5.1 | 7.5 | 6.3 |
| Altarani | DS | 15.3 | 23.5 | 19.4 | 0.7 | 0.7 | 0.7 | 4.7 | 47.1 | 25.9 | 3 | 21.6 | 12.3 | 0.4 | 4.8 | 2.6 | 1.7 | 2.1 | 1.9 | 3.1 | 11.1 | 7.1 |
| | WS | 15.3 | 22.1 | 18.7 | 0.5 | 1.3 | 0.9 | 4.6 | 6.4 | 5.5 | 3.5 | 4.5 | 4 | 0.7 | 0.9 | 0.8 | 1.5 | 1.7 | 1.6 | 3.8 | 4.2 | 4 |
| Asana 2 | DS | 16.1 | 24.7 | 20.4 | 0.7 | 1.1 | 0.9 | 32.2 | 37.6 | 34.9 | 9 | 21.6 | 15.3 | 1.6 | 6.2 | 3.9 | 1.6 | 3.4 | 2.5 | 4.9 | 12.5 | 8.7 |
| | WS | 17.2 | 22.8 | 20 | 0.6 | 0.8 | 0.7 | 26.4 | 43.8 | 35.1 | 11 | 14.2 | 12.4 | 1.9 | 3.3 | 2.6 | 1.7 | 2.3 | 2 | 5.5 | 6.3 | 5.9 |
| Asana 3 | DS | 3.2 | 30 | 16.6 | 1 | 1.2 | 1.1 | 40.7 | 54.1 | 47.4 | 15 | 19.4 | 17 | 2.5 | 5.1 | 3.8 | 2 | 3 | 2.5 | 5.3 | 12.3 | 8.8 |
| | WS | 4.9 | 15.1 | 10 | 0.5 | 1.7 | 1.1 | 45.8 | 66.4 | 56.1 | 14 | 17.2 | 15.4 | 2.7 | 4.1 | 3.4 | 2.4 | 2.4 | 2.4 | 6.6 | 7.4 | 7 |
| Asana 4 | DS | 6.9 | 29.9 | 18.4 | 0.7 | 2.7 | 1.7 | 47.1 | 56.1 | 51.6 | 13 | 19.8 | 16.5 | 2.7 | 4.5 | 3.6 | 2.1 | 2.5 | 2.3 | 5.7 | 10.3 | 8 |
| | WS | 12.3 | 13.1 | 12.7 | 0.4 | 4 | 2.2 | – | – | – | 13 | 16.5 | 14.8 | 2.3 | 3.9 | 3.1 | 2.3 | 2.7 | 2.5 | 6.5 | 7.1 | 6.8 |
| Charaque | DS | 19.5 | 26.5 | 23 | 1.2 | 2.6 | 1.9 | 12.8 | 16 | 14.4 | 6.9 | 11.9 | 9.4 | 1.5 | 4.1 | 2.8 | 2.6 | 3.2 | 2.9 | 4.5 | 9.1 | 6.8 |
| | WS | 23.5 | 29.5 | 26.5 | 1.3 | 2.1 | 1.7 | 13.1 | 16.7 | 14.9 | 6.4 | 7 | 6.7 | 2 | 2.2 | 2.1 | 2.5 | 3.3 | 2.9 | 5 | 5.8 | 5.4 |
| Capillune | DS | 60.8 | 111 | 85.9 | 54.7 | 489 | 271.9 | 137 | 411 | 274 | 46 | 175 | 110.3 | 1.7 | 19.1 | 10.36 | 0.6 | 10 | 5.34 | 71 | 259 | 165.1 |
| | WS | 109 | 120 | 114.9 | 225 | 692 | 458.5 | 174 | 784 | 478.8 | 80 | 281 | 180.6 | 11 | 28.5 | 19.8 | 6.1 | 7.7 | 6.9 | 141 | 431 | 286.2 |
| Tumilaca | DS | 27.6 | 78.2 | 52.9 | 5.1 | 17.5 | 11.3 | 47.6 | 139 | 93.5 | 19 | 37.8 | 28.3 | 3.6 | 6 | 4.8 | 2.2 | 3.2 | 2.7 | 14 | 22.1 | 18 |
| | WS | 65.6 | 80 | 72.8 | 12.6 | 18.6 | 15.6 | 70 | 76 | 73 | 34 | 45.4 | 39.8 | 4.3 | 6.1 | 5.2 | 2.1 | 3.9 | 3 | 18 | 23.4 | 20.8 |
| WQS Cat 4 River OMS Global average* | | | 52 | | | 5.5 | | | 8.9 | | | 14.4 | | | 4 | | | 1.2 | | | 5.4 | |

DS: dry season April–December, WS: wet season January–March. *
Source: Tsering et al. [30]. Ca = total calcium, Mg = total magnesium, K = total potassium, Na = total sodium.

**Table 3**
Metal content in sediments at monitoring stations in the Asana-Tumilaca Basin during the dry (2013, 2017, and 2020) and wet (2014, 2018, and 2019) seasons.

| Monitoring stations | | As | | | Hg | | | Cd | | | Cu | | | Cr | | | Pb | | | Zn | | |
|---|---|---|---|---|---|---|---|---|---|---|---|---|---|---|---|---|---|---|---|---|---|---|
| | | mg/L | | | | | | | | | | | | | | | | | | | | |
| | | Min | Max | Mean | Min | Max | Mean | Min | Max | Mean | Min | Max | Mean | Min | Max | Mean | Min | Max | Mean | Min | Max | Mean |
| Asana 1 | DS | <0.4 | <0.4 | <0.4 | <0.02 | <0.02 | <0.02 | <0.03 | 3.88 | 1.94 | 17.9 | 36.84 | 27.37 | 9.55 | 17.5 | 13.52 | <0.4 | 8.42 | 4.41 | 36.4 | 59.4 | 47.85 |
| | WS | <0.4 | 3.3 | 1.12 | <0.02 | 1 | 0.05 | <0.03 | 2.27 | 0.77 | 15.6 | 31.8 | 21.1 | 8.81 | 11.9 | 10.59 | <0.4 | 7.53 | 4.04 | 36.7 | 42 | 40 |
| Altarani | DS | <0.4 | 4.2 | 1.4 | <0.02 | <0.02 | <0.02 | <0.03 | 10.7 | 3.65 | 25.8 | 26.6 | 26.18 | 7.9 | 62.5 | 29.45 | 12.4 | 15.1 | 13.38 | 41.3 | 85.4 | 61.76 |
| | WS | <0.4 | 2.6 | 1.69 | <0.02 | <0.02 | <0.02 | <0.03 | 1.26 | 0.51 | 20 | 42.15 | 28.85 | 7.39 | 14.4 | 9.8 | 10.7 | 25.5 | 16.46 | 27.8 | 48.9 | 37.03 |
| Asana 2 | DS | <0.4 | <0.4 | <0.4 | <0.02 | <0.02 | <0.02 | <0.03 | 4.58 | 2.29 | 24.4 | 46.55 | 35.45 | 20.9 | 22.4 | 21.67 | 13.5 | 20.1 | 16.81 | 51.9 | 83.6 | 67.76 |
| | WS | <0.4 | <0.4 | <0.4 | <0.02 | <0.02 | <0.02 | <0.03 | 0.16 | 0.08 | 18.9 | 57.24 | 38.07 | 12.4 | 13.2 | 12.78 | <0.4 | 10.8 | 5.6 | 37.7 | 47.6 | 42.65 |
| Asana 3 | DS | <0.4 | <0.4 | <0.4 | <0.02 | <0.02 | <0.02 | <0.03 | 4 | 2 | 48.5 | 169.4 | 109 | 22.6 | 93.3 | 57.96 | 10.8 | 14.2 | 12.5 | 45.1 | 52.4 | 48.71 |
| | WS | <0.4 | 2.6 | 0.96 | <0.02 | <0.02 | <0.02 | <0.03 | 1.49 | 0.51 | 31 | 130.5 | 94.71 | 7.81 | 73.8 | 29.99 | 6.44 | 10.6 | 8.34 | 33.2 | 39.7 | 37.3 |
| Asana 4 | DS | <0.4 | 13 | 4.33 | <0.02 | <0.02 | <0.02 | <0.03 | 1.99 | 0.88 | 33.3 | 166.6 | 116.6 | 7.72 | 126 | 51.93 | 12.4 | 61.8 | 31.49 | 38.6 | 227 | 104.7 |
| | WS | <0.4 | <0.4 | <0.4 | <0.02 | <0.02 | <0.02 | <0.03 | 0.16 | 0.08 | 160 | 186.3 | 173 | 3.45 | 7.1 | 5.27 | 6.15 | 18.9 | 12.52 | 39.2 | 40.5 | 39.86 |
| Charaque | DS | <0.4 | 2.3 | 1.77 | <0.02 | <0.02 | <0.02 | <0.03 | 2.41 | 0.84 | 30.1 | 38.2 | 35.04 | 5.9 | 36.8 | 18.12 | 5.46 | 17.4 | 10.54 | 29.5 | 42.7 | 34.6 |
| | WS | <0.4 | 3.22 | 1.61 | <0.02 | <0.02 | <0.02 | <0.03 | 1.27 | 0.47 | 27.7 | 52.8 | 42.27 | 3.7 | 52.8 | 20.68 | 7.49 | 14.2 | 11.76 | 19.3 | 35.9 | 32.72 |
| Capillune | DS | <0.4 | 6.6 | 2.2 | <0.02 | <0.02 | <0.02 | <0.03 | 2.26 | 0.8 | 15.3 | 37.9 | 24.57 | 1.9 | 6.69 | 4.64 | 3.69 | 24.3 | 11.84 | 33 | 57 | 48.41 |
| | WS | <0.4 | 3.91 | 2.57 | <0.02 | <0.02 | <0.02 | <0.03 | 2.46 | 0.87 | 19.5 | 30.2 | 23.46 | 3.21 | 10.2 | 6.25 | 8.07 | 66.2 | 30.31 | 28.7 | 44.8 | 37.08 |
| Tumilaca | DS | <0.4 | <0.4 | <0.4 | <0.02 | <0.02 | <0.02 | <0.03 | 3.54 | 1.77 | 73.3 | 97.05 | 85.18 | 11.7 | 15 | 13.36 | 9.46 | 16 | 12.73 | 41.5 | 75.9 | 58.69 |
| | WS | <0.4 | 5.8 | 1.65 | <0.02 | <0.02 | <0.02 | <0.03 | 1.62 | 0.33 | 32.3 | 119.2 | 95.42 | 2.76 | 8.5 | 4.68 | 3.46 | 7.95 | 5.71 | 21.4 | 38 | 37.14 |
| ISQG | | 5.9 | | | | 0.17 | | 0.6 | | | 35.7 | | | 37.3 | | | 35 | | | 123 | | |
| PEL | | 17 | | | | 0.486 | | 3500 | | | 197 000 | | | 90 | | | 91.3 | | | 315 | | |

DS: dry season April–December, WS: tweet season January–March.

multivariate statistical techniques for reducing the parameters in environmental indices [26], enabling the reduction of extensive data matrices into a limited number of factors [27]. Through PCA, the analysis incorporated PPW, MCS, and hydrobiological diversity indices, all of which are linked to factors such as runoff, precipitation, groundwater influx, anthropogenic contamination, and soil erosion in snow-covered areas, among others [28,29].

## 3. Results and discussion

### 3.1. Physicochemical composition of water (PPW)

Analyzing the relationship and trends among various PPW plays a crucial role in understanding environmental conditions and their potential impacts on aquatic ecosystems. Hence, the focus of this study was examining the relationship and trends among electrical conductivity (EC), dissolved oxygen (DO), pH, temperature, and ions like bicarbonates, chlorides, sulfates, sodium, potassium, calcium, and magnesium. These ions exert significant effects on water quality and aquatic life.

Tables 1 and 2 show the results of PPW using the minimum, maximum, and mean values for each river in the basin, and Fig. 3a shows the total values for each parameter. The temperature in the Asana-Tumilaca Basin fluctuated between 10.0 and 18.6 °C during the dry and wet seasons. The rivers Asana (monitoring stations Asana 1, Asana 2, Asana 3, and Asana 4), Altarani, and Charaque, situated in the upper part of the basin (ranging from 3908 to 2500 masl), recorded the lowest temperature values, varying between 10 and 14.7 °C. These values were attributed to the particular environmental conditions of the high Andean region. In contrast, the Tumilaca River, located in the lower part of the basin (1680 masl), exhibited higher temperature values, ranging from 15.6 to 17.3 °C, mainly due to its proximity to the Moquegua Valley. Conversely, the Capillune River (2850 masl) displayed the highest temperature values, ranging from 18.4 to 18.6 °C, due to the influence of geothermal waters from the area known as "Calientes." Elevated temperatures promote evaporation, which adversely affects hydrobiological richness, as was the case for the Capillune River. Furthermore, moderate temperatures, combined with intense solar radiation fostered an increase in richness, although not in diversity, which is

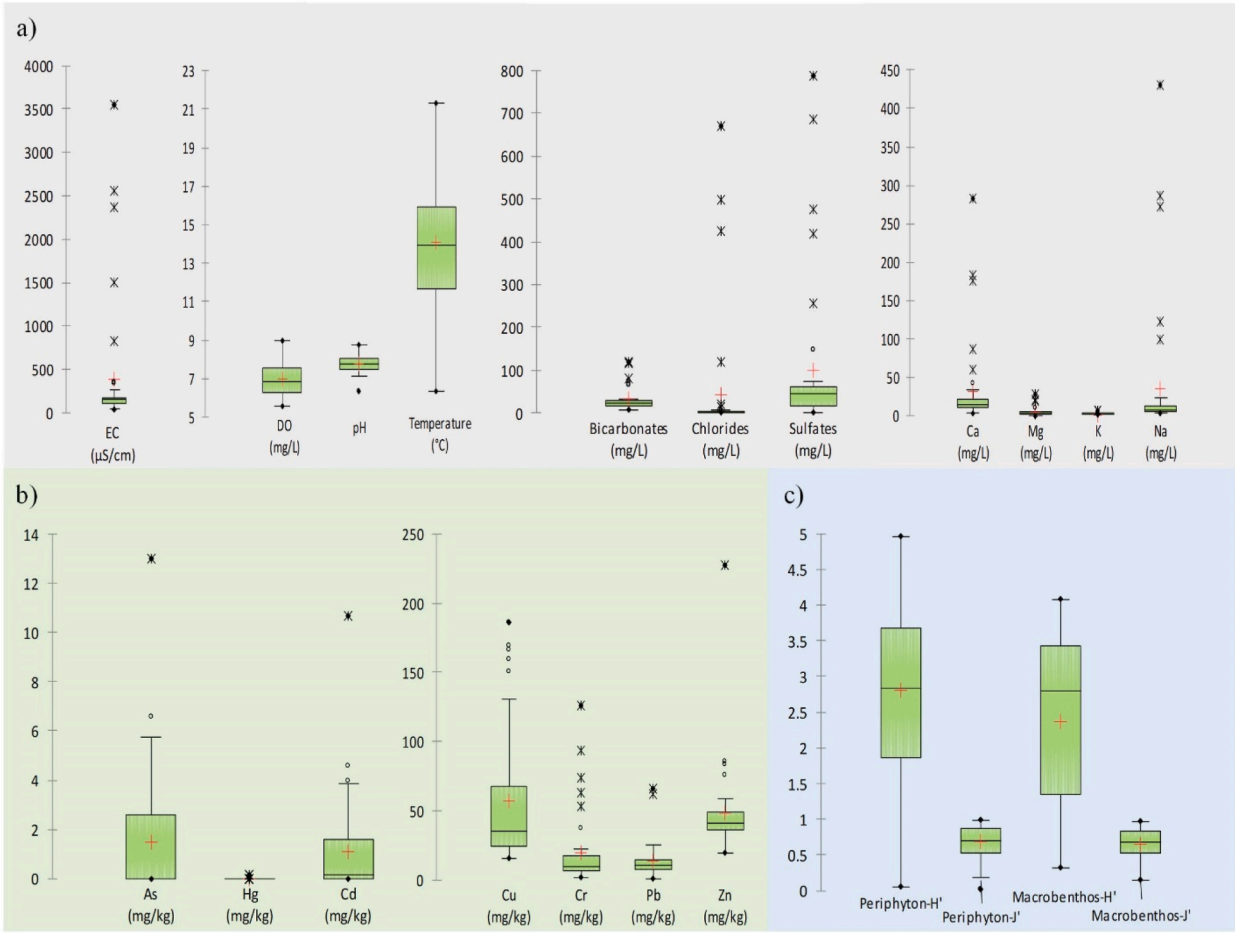


**Fig. 3.** Box-plot presentation of the global variability in a) physicochemical parameters of water, b) metal content in sediments, c) hydrobiological diversity indices in the Asana-Tumilaca Basin.

attributed to the higher proliferation of photosynthetic microorganisms, as observed in the Tumilaca River.

Throughout the dry and wet seasons, DO levels fluctuated within the range of 6.5–8.2 mg/L. In the dry season, the Tumilaca River exhibited the highest DO concentration at 7.9 mg/L, whereas during the wet season, the Asana 4 and Tumilaca Rivers had concentrations of 8.0 and 8.2 mg/L, respectively. This increase in the DO concentration is linked to increased photosynthetic processes driven by intense solar radiation [8].

The pH values in the Asana-Tumilaca Basin ranged from 7.1 to 8.4 during both dry and wet seasons. The Tumilaca and Capillune Rivers exhibited the highest pH values, reaching 7.8 and 8.3, and 8.3 and 8.4, respectively, during the dry and wet seasons. In both rivers, elevated pH was linked to increased bicarbonate concentrations. Additionally, in the case of the Tumilaca River, higher pH levels were associated with enhanced photosynthesis. EC values ranged from 60 to 2446 μS/cm in the dry and wet seasons. The highest EC values were found in the Capillune River, reaching 1575 μS/cm during the dry season and 2446 μS/cm during the wet season. This phenomenon was attributed to the influx of geothermal water into the Capillune River, causing water evaporation and subsequent ion concentration. Similar results were reported by Pandey et al. [6]. Consequently, this process had a detrimental impact on the hydrobiological richness in the study area, as evidenced by the reduction in hydrobiological richness during both seasons (Fig. 4a and b), which were also reported by Reid et al. [31].

The waters of the Asana and Tumilaca Rivers are categorized as calcium sulfate waters, whereas those of the Capillune River are sodium and magnesium chloride sulfate waters. In contrast, the Altarani and Charaque Rivers exhibit properties of calcium bicarbonate water, as shown in the Piper diagram (Fig. 4); results similar were reported by Visitación et al. [8]. Notably, there are no distinct variations in river water classifications between the dry and wet seasons. Additionally, according to the Wilcox index, the water quality was classified as very good (C1S1) for the Asana, Charaque, and Altarani Rivers, good (C2S1) for the Tumilaca River, and poor (C4S1 and C4S2) for the Capillune River (Fig. 5a and b) [6].

The prevailing ions in the river basin were Ca, Na, and sulfates. The decreasing order of cations is Ca > Na > Mg > K, and for anions, it followed the sequence sulfates > bicarbonates > chlorides. Cations Ca and Na collectively contribute 81.4%, which is consistent with that of Tsering et al. [30]. Similarly, anions sulfates and bicarbonates constituted 95.8% of the total. The presence of sulfates in rivers primarily results from the dissolution of sulfated sedimentary minerals, weathering of sulfurous sedimentary minerals, and volcanic emissions [32]. In the upper reaches of the basin, the concentration of Ca and Mg ions in the Asana, Altarani, and Charaque rivers were higher during the dry season than during the wet season because of dilution processes in the wet season and concentration in the dry season. The elevated ion concentration in the Capillune River has been attributed to the inflow of geothermal water or groundwater (classified by INGEMMET as a volcanic fractured Barroso aquifer), water evaporation processes, and ion concentrations. The Tumilaca River exhibited the highest ion concentration of Na compared to the Asana, Altarani, and Charaque Rivers, owing to ion contributions from the soil in the proximity of the valley and the influence of groundwater. Furthermore, the elevated concentrations of anions and cations in the Capulline and Tumilaca Rivers, when compared to the global mean (Table 2), provide further evidence of the distinctive nature of subsurface water.

In the upper region of the basin, specifically in the Asana rivers (Asana 1, Asana 2, Asana 3, and Asana 4), Altarani, and Charaque, the concentrations of bicarbonate, chloride, and magnesium ions were below the global mean. In contrast, the concentrations of sulfate, potassium, and calcium ions exceeded this mean, as reported by Tsering et al. [30]. This variation can be attributed to the presence of sulfated minerals such as alunite $KAl_3(SO_4)_2(OH)_6$ [8,33], which generate acidity that is subsequently neutralized by bicarbonates. In the lower part of the Tumilaca River, the concentrations of bicarbonate, chloride, sulfate, calcium, magnesium,

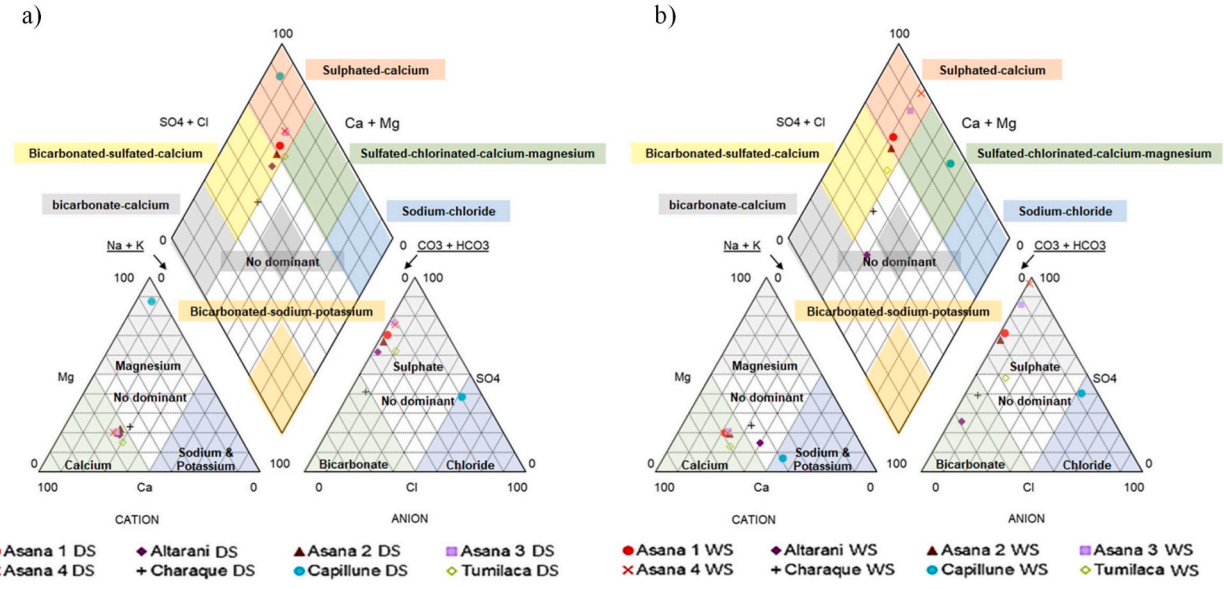


**Fig. 4.** Piper diagram of the water from the monitoring points in the Asana-Tumilaca Basin during the a) dry season (DS) and b) wet season (WS).

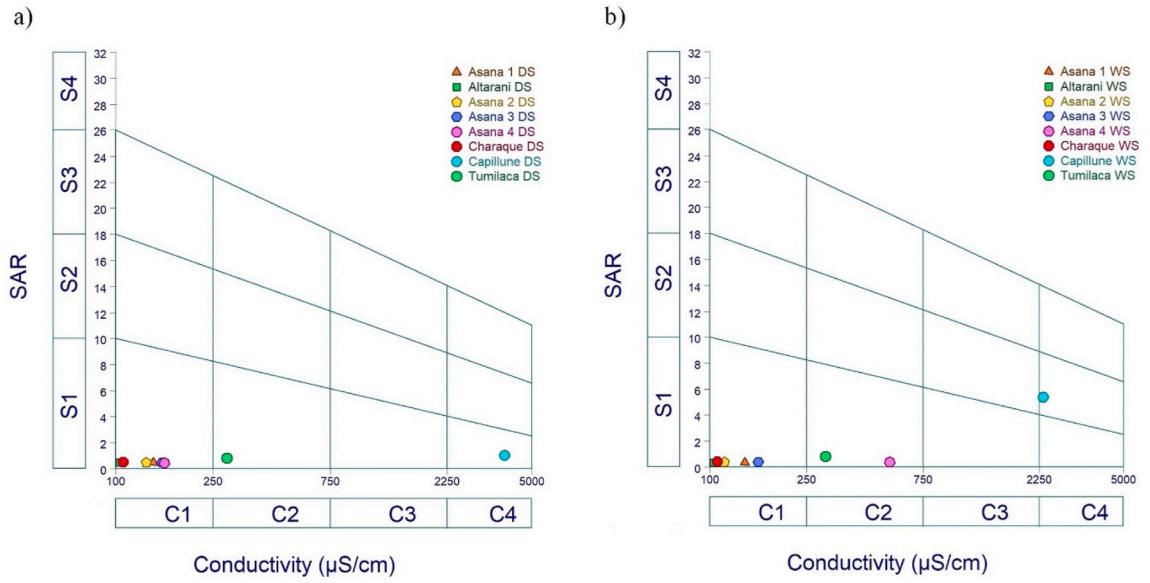


**Fig. 5.** The river water classification of the Asana-Tumilaca Basin according to the Wilcox diagram at the monitoring stations during the a) dry season (DS) and b) wet season (WS).

potassium, and sodium ions were higher than the global mean because of the influx of groundwater and soil leaching typical of the valley area. Meanwhile, in the case of the Capillune River, the excess over the global mean can be attributed to the inflow of geothermal water and reduced flow, leading to ion concentrations.

Higher ion content in the water enhances the diversity and evenness of periphyton, but not its hydrobiological richness, particularly during the dry season when water flow is limited. Conversely, high ion concentrations reduced the diversity and evenness of macrobenthos, particularly during the dry season.

### *3.2. Metal content in sediments (MCS)*

The MCS using the minimum, maximum, and mean values for each river in the basin are reported in Table 3, and the total values for each metal are shown in Fig. 3b. The mean values varied as follows: Cu (172.98 mg/kg) > Zn (104.73 mg/kg) > Cr (57.96 mg/kg) > Pb (31.49 mg/kg) > As (4.33 mg/kg) > Cd (3.65 mg/kg) > Hg (0.05 mg/kg) (Table 3). Notably, the Cd, Cu, and Cr levels exceeded the ISQG, suggesting potential harm to aquatic organisms. Cd concentrations remained relatively stable across the basin during the dry and wet seasons. In contrast, elevated Cu levels were observed in the lower section of the Asana River (Asana 3 and Asana 4), and the Charaque and Tumilaca Rivers exhibited high Cu values.

The sediment samples in the basin exhibited a range of mean metal concentrations: As (from <0.4 to 4.33 mg/kg), Hg (from <0.02 to 0.05 mg/kg), Cd (from 0.08 to 3.65 mg/kg), Cu (from 21.1 to 172 mg/kg), Cr (from 4.64 to 57.96 mg/kg), Pb (from 4.04 to 31.49 mg/kg), and Zn (from 32.72 to 104.73 mg/kg). These concentrations are consistent with the natural levels found in the Earth's crust: 1.8 mg/kg for As, 0.08 mg/kg for Hg, 0.2 mg/kg for Cd, 55 mg/kg for Cu, 100 mg/kg for Cr, 12.5 mg/kg for Pb, and 70 mg/kg for Zn [34]. This suggests that the metals in the study area have a natural origin, likely resulting from processes such as rock erosion, surface runoff [8], and susceptibility to soil mass movements in the study area [35]. The mean concentration of As in the sediment remained within the ISQG limits throughout the dry and wet seasons at all monitoring stations. The highest concentrations were observed during the dry season at the lowest monitoring station along the Asana River (Asana 4). This increase can be attributed to the groundwater inflow during periods of low water flow, which promotes heightened sedimentation and deposition of soil material. The Hg concentration was detected only during the wet season at monitoring station Asana 1 and did not exceed the ISQG threshold. In contrast, the Cd concentration exceeded the ISQG values at all monitoring stations during the dry season. This can be primarily attributed to the bioaccumulation of Cd in plankton, followed by its deposition in seabed sediment and soil exposure during the formation of mountain chains [36], a common occurrence in Peruvian soils. Cu concentrations in the sediment at all monitoring stations surpass the ISQG thresholds, primarily because of the geological abundance of this metal in the Moquegua region. Additionally, Cu levels were higher during the wet season, influenced by runoff that transports soil material to the riverbed [11]. Likewise, the Cr concentration in the sediment exceeded the ISQG value at Asana 3 and Asana 4 stations during the dry season, mirroring the trend observed for Cu. Furthermore, Pb and Zn concentrations were typically lower than the ISQG limits and tended to increase during the dry season, showing a clear correlation with As concentration. At low concentrations, Cu and Zn play crucial roles in biological systems. In contrast, Cd, As, Hg, and Pb are nonessential heavy metals [37]. Notably, Pb and Cd are highly toxic to the biota [38].

### 3.3. Monitoring of glacier melting zones

In the Asana-Tumilaca Basin, the rivers originate from two snow-capped mountains, Arundane and Chuquiananta. These mountains play crucial roles in shaping the basin's PPW, water availability, MCS, and hydrobiological diversity, particularly at the higher-altitude monitoring stations, Asana 1 and Altarani. The snow cover on Arundane fluctuated from 0.1 to 0.3 $km^2$ during the dry season and expanded to 1.5–3.0 $km^2$ in the wet season (Fig. 6a and b). Meanwhile, in Chuquiananta, the coverage ranged from 1.1 to 2.0 $km^2$ during the dry season and extended to 0.5–10.5 $km^2$ in the wet season (Fig. 6a and b). Díaz et al. [39] and Monge et al. [40] reported similar values.

The most significantly thawed areas recorded between the dry season of 2017 and the wet season of 2018 in the Arundane mountain covered 2.7 $km^2$. In Chuquiananta, from the wet season of 2019 to the dry season of 2020, the thawed area extended to 9 $km^2$. Conversely, the smallest thawed areas for both mountains, observed between the dry season of 2013 and the wet season of 2014, were <1 $km^2$. A larger thawed area amplifies soil erosion and introduces mineral elements that influence the PPW and MCS [41]. Furthermore, increased water flow carrying suspended particles results in the detachment of periphyton from rocks owing to shear stress and abrasion, impacting the hydrobiological diversity of water bodies in the Asana-Tumilaca Basin.

### 3.4. Monitoring of hydrobiological community

The hydrobiological diversity indices of periphyton were higher during the initial years of monitoring. The Shannon-Wiener index (H′) during the dry season followed the order of 2013 > 2017>2020, and during the wet season it was 2014 > 2018>2019. Similarly, the Pielou's evenness index (J′) trend during the dry season followed the order of 2017 > 2013>2020, and during the wet season, it was 2014 ≅ 2018>2019 (Fig. 7). The H′ diversity values during the dry season ranged from 0.74 to 4.66, with a mean of 2.62, indicating a low to high level of diversity. In the wet season, H′ values ranged from 0.05 to 4.94, with a mean of 2.88, suggesting a similar level of diversity of means (Fig. 3c), with better environmental conditions for the wet season, in agreement with that reported by Ochieng et al. [14]. Moreover, the J′ values during the dry season ranged from 0.23 to 0.97, with a mean of 0.68, and in the wet season, they ranged from 0.01 to 0.99, with a mean of 0.70. These mean values indicate that all species have equal evenness, and Ochieng et al. [14] reported the same trend between the dry and wet seasons, although with lower evenness values. The periphyton richness values during the dry season ranged from 16 to 67, with a mean of 34, whereas during the wet season, they ranged from 7 to 81, with a mean of 36.

During the dry season, a decline in the diversity index and a reduction in periphyton richness were observed over time, with an inconsistent trend in the evenness index. The decrease in diversity and evenness indices in 2020 could be linked to human activity, shifts in nutrient quantities and types, and physical modifications in rivers that alter their structure and function [42]. During the wet

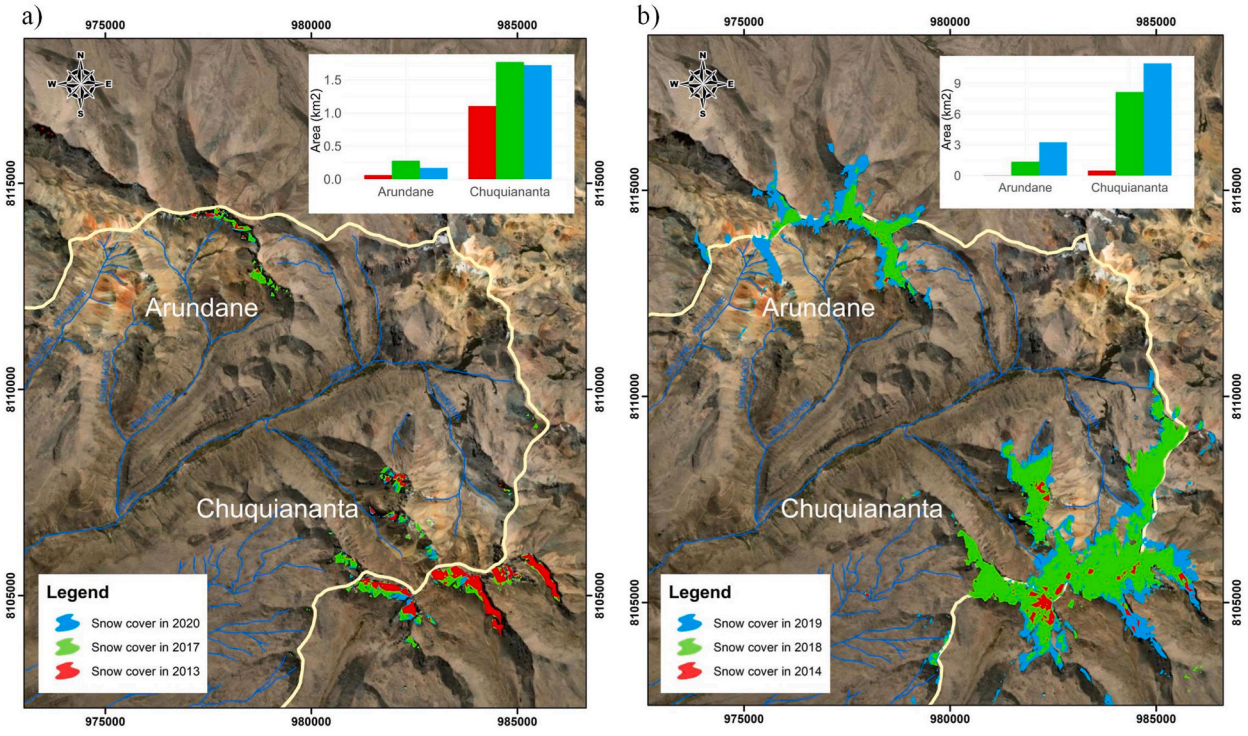


**Fig. 6.** Monitoring of snow cover in the Arundane and Chuquiananta mountain ranges during the a) dry season (DS) and b) wet season (WS).

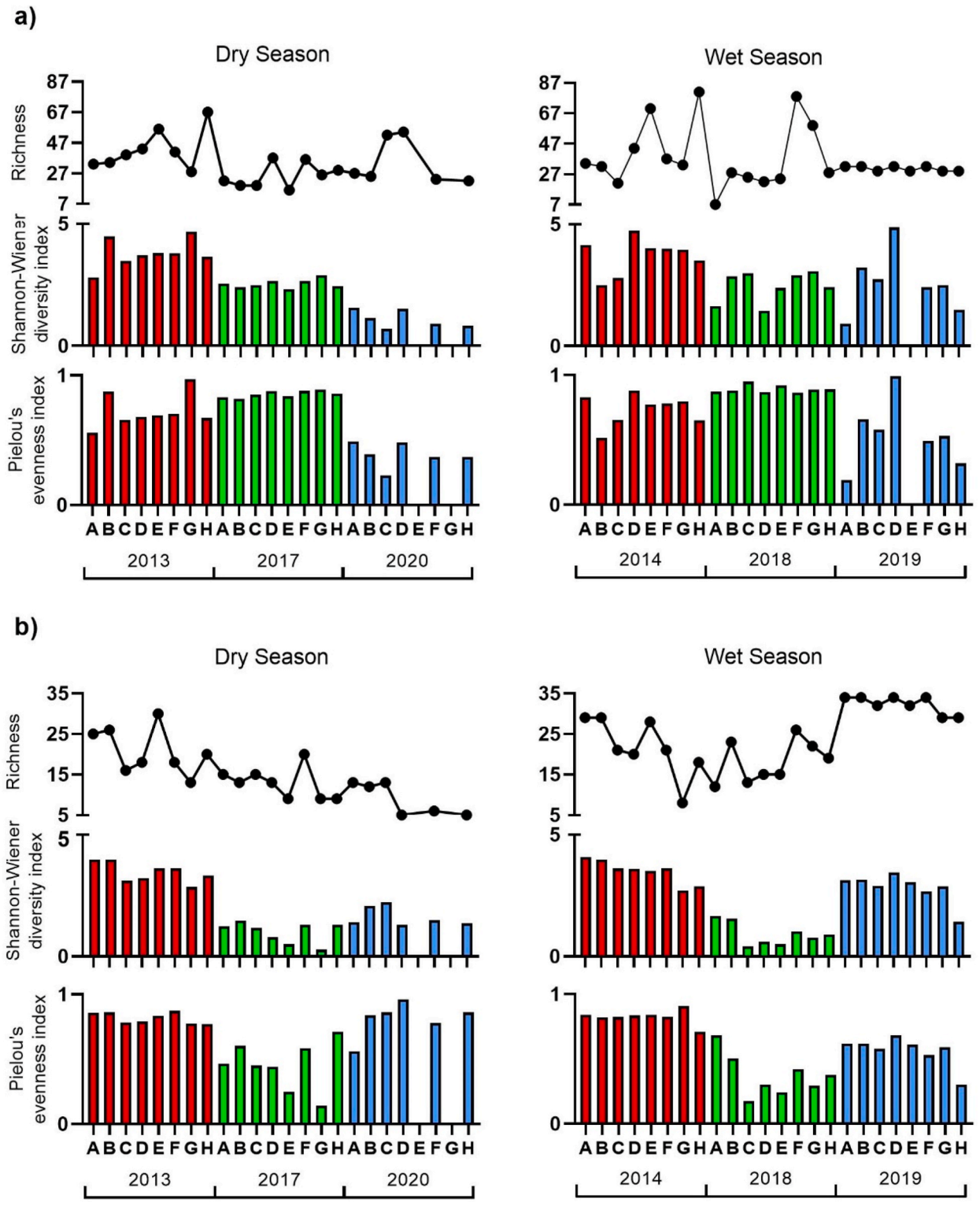


**Fig. 7.** Shannon-Wiener diversity indices, Pielou's evenness, and richness of a) periphyton and b) macrobenthos at the monitoring stations Asana 1 (A), Altarani River (B), Asana 2 River (C), Asana 3 River (D), Asana 4 River (E), Charaque River (F), Capillune River (G), and Tumilaca River (H).

season, a fluctuating pattern in diversity and evenness indices, and in richness, was encountered, with lower values observed in 2019 across the board. This fluctuation is likely a result of increased precipitation, which leads to alterations in physicochemical parameters, higher flow rates, and the presence of suspended solids. These factors diminish light penetration into the riverbed, causing shear stress and rock abrasion, and ultimately affecting periphyton diversity [2,43].

The hydrobiological diversity indices for macrobenthos exhibited a variable pattern, with the lowest values recorded in 2017. The Shannon–Wiener index (H′) during the dry season followed the order of 2013 > 2020>2017, and during the wet season it was 2014 > 2019>2018. Similarly, the Pielou's evenness index (J′) trend during the dry season followed the order of 2013 ≅ 2020>2017 and during the wet season it was 2014 > 2019>2018 (Fig. 7). The H′ diversity values during the dry season ranged from 0.31 to 3.99, with a mean of 2.10, indicating a low to high level of diversity. In the wet season, the H′ values ranged from 0.45 to 4.08, with a mean of 2.44, suggesting a similar level of diversity. This trend was also reported by Venarsky et al. [44], who reported that macrobenthos opted for strategies such as osmoregulation and burrowing into the sediment that allow them to maintain their abundance over time. Moreover, the Pielou's evenness index (J′) values during the dry season ranged from 0.14 to 0.96, with a mean of 0.68, and during the wet season, they varied from 0.18 to 0.91, with a mean of 0.59. These mean values indicate that all species had similar evenness, although equity was lower during the wet season because large-bodied and long-lived benthic communities predominated [44]. Macrobenthos richness ranged from 5 to 30 during the dry season, with a mean of 15, and from 8 to 34 during the wet season, with a mean of 24. Richness and diversity (H′) values during the dry season decreased over time, whereas the evenness index (J′) remained relatively constant. Similarly, during the wet season, the richness values displayed a fluctuating pattern, with lower values recorded in 2018. This trend was also evident in diversity and evenness indices.

During the dry season, a consistent decrease in both macrobenthic diversity and richness was observed over time, along with a fluctuating pattern in the evenness index, which was also reported by Venarsky et al. [44]. This decline in diversity likely resulted from anthropogenic activities that reshaped the structure and function of rivers [42]. During the wet season, variable values for the diversity, evenness, and richness indices were encountered, with lower values uniformly recorded in 2018. This variation likely resulted from increased precipitation, which in turn affects physicochemical parameters, including heightened flow rates and water volume [43].

As show in Fig. 7a, during the 2018 wet season, there were noticeable variations in the diversity index for periphyton among monitoring stations Asana 1 (1.70), Altarani (2.93), and Asana 2 (3.06), which are categorized as "moderate diversity". Notably, the evenness index remained relatively consistent across these monitoring stations. Additionally, richness values increased progressively from Asana 1 (7) to Altarani (28) and Asana 2 (25). These variations in diversity and richness resulted from the geographical location of the rivers. Asana 1, situated at the highest station on the Asana River, is directly affected by glacial melt, which leads to a sudden surge in water flow and soil erosion, releasing sulfate ions and other metals that increase overall EC [8]. These factors collectively influence periphyton diversity and richness [31]. This trend diminishes as it moves downstream in the basin, as seen in Asana 2, which is located downstream of the confluence of the Asana and Altarani rivers.

During the dry season of 2013, a similar pattern in the diversity index for periphyton was observed between Asana 1 and Altarani monitoring stations, with Asana 1 categorized as having 'moderate diversity' (2.80) and Altarani as having 'high diversity' (4.45). In contrast, during the wet season of 2019, Asana 1 exhibited 'low diversity' (0.97), whereas Altarani showed 'high diversity' (3.28), similar to reported by Ochieng et al. [14]. In Fig. 7b, focusing on macrobenthos during the dry season of 2020, variations in the diversity index are evident among Asana 1, Altarani, and Asana 2, classified as "low diversity" (1.43), "moderate diversity" (2.10), and "moderate diversity" (2.26), respectively. The evenness index was rated as "moderate" (0.56) for Asana 1 and "good" for Altarani and Asana 2 (0.84 and 0.86, respectively). These variations are linked to glacial melt, causing soil erosion and the accumulation of salts, which subsequently increases EC and restricts greater diversity in Asana 1, as reported by Reid et al. [31].

As shown in Fig. 7a, during the wet season of 2019, a striking contrast was evident between the diversity indices of periphyton at the Asana 3 and Asana 4 monitoring stations. Asana 3 was characterized by 'high diversity' (4.95), whereas Asana 4 exhibits 'low diversity' (0.05). Additionally, the evenness index for Asana 3 was rated as 'good' (0.99), whereas Asana 4 was classified as 'poor' (0.01). This notable divergence was primarily attributed to anthropogenic activities involving land excavation between the two monitoring stations; Aziz et al. [24] reported a similar trend in fiches. Such activities result in an increase in metal concentrations in the sediment, including those of Cu and other metals. In particular, Cu has a significant impact on the development and growth of periphyton, which accumulates within these organisms [45]. Notably, this discrepancy was not mirrored in the macrobenthos diversity indices (Fig. 7b).

In Capillune, a monitoring station near the "Calientes" area, during the 2013 and 2017 dry seasons and the 2014 wet season, macrobenthos richness values were 13, 9, and 8, respectively (Fig. 7b). These values were notably lower than those of the other monitoring stations, including Asana 1, Altarani, Asana 2, Asana 3, Asana 4, and Charaque. This behavior is attributed to the presence of geothermal waters in this area, which leads to elevated temperatures, water evaporation, and a higher salt concentration, subsequently increasing the EC. However, this trend did not affect periphyton richness during the studied seasons [6,31].

In Tumilaca, a monitoring station located at the entrance of the Moquegua Valley, during the 2013 dry season and 2014 wet season, the periphyton richness values were 67 and 81, respectively (Fig. 7a). These values were higher than those of other monitoring stations, including Asana 1, Altarani, Asana 2, Asana 3, Asana 4, and Charaque, while maintaining high diversity indices (3.64 and 3.59) and good evenness (0.67 and 0.65); Zhao et al. [46] also reported this trend. This behavior is attributed to the favorable environmental conditions in the valley, which are characterized by high temperatures and high UV radiation. These factors positively influence the photosynthetic processes of organisms such as periphytons. Conversely, during the 2020 dry season and the 2019 wet season, the diversity index classification was notably lower, categorized as "low diversity" (0.86 and 1.55), and evenness is considered "poor" (0.37 and 0.32). This change was due to the release of wastewater from anthropogenic activities in the valley, which promoted the growth of

certain microorganisms and reduced the diversity and evenness indices of periphyton, a similar trend was reported by Panja et al. [21]. Additionally, a similar pattern was observed during the wet season of 2019, with a classification of "low diversity" (1.45) and "poor evenness" (0.30) for macrobenthos.

Fig. 8a, b shows the taxonomic composition of aquatic organisms in periphyton. Notably, microalgae from the phylum Ochrophyta dominate during the 2013 and 2020 dry seasons and the 2014 and 2019 wet seasons. Conversely, microalgae from the phylum Bacillariophyta were dominant during the 2017 dry season and 2018 wet season. Both phyla exhibited adaptability to various conditions, including changes in flow, current velocity, and the presence of metals and organic matter, among other factors.

Ochrophyta and Bacillariophyta have demonstrated a greater capacity to bioaccumulate As than other algal types [45]. This ability likely accounts for their prevalence at monitoring stations. Regarding the taxonomic composition of aquatic organisms in macrobenthos, arthropods have emerged as the dominant group and play a significant role in aquatic ecosystems. Many arthropods demonstrate resilience to environmental changes within their habitats and occupy diverse ecological niches [43,47,48].

The results of the efficiency indicators of the predictive model are presented in Table 4. These results comply with a normal distribution and homogeneity of variance of the residuals, for the diversity (periphyton-H′ and macrobenthos-H′) and evenness indices (periphyton-J′ and macrobenthos-J′) for the three cases. The efficiency of the prediction model for hydrobiological diversity and evenness indices increased in the following order: case 1 (based on PPW data) < case 2 (based on MCS data) < case 3<(based on PPW and MCS data). Moreover, the results for macrobenthos were better than for periphyton, the correlation values (R) between the observed value and the estimated diversity (H′) and equity (J′) were 0.87 to 0.73, with minimum RMSE values of 0.58 and 0.16,

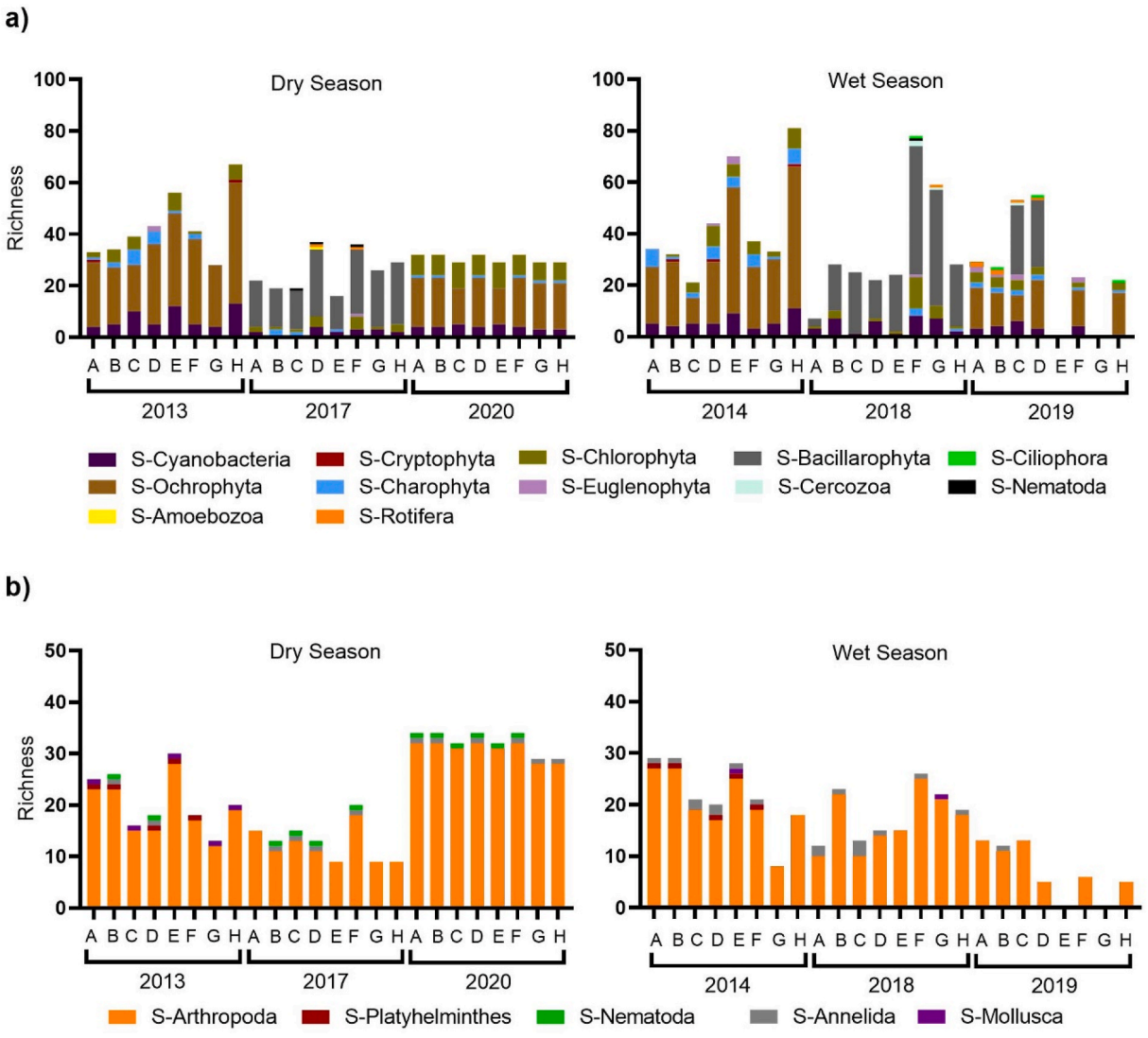


**Fig. 8.** Taxonomic composition of a) periphyton and b) macrobenthos at the monitoring stations Asana 1 (A), Altarani River (B), Asana 2 River (C), Asana 3 River (D), Asana 4 River (E), Charaque River (F), Capillune River (G), and Tumilaca River (H).

**Table 4**
Performance of the models in prediction of hydrobiological diversity indices for cases 1 to 3.

| Performance indicators | Variables | | | |
|---|---|---|---|---|
| | Periphyton-H′ | Periphyton-J′ | Macrobenthos-H′ | Macrobenthos-J′ |
| Case 1 | | | | |
| RMSE | 1.2358 | 0.2268 | 0.9998 | 0.2009 |
| Sd | 0.4950 | 0.1176 | 0.8513 | 0.1456 |
| $R^2$ | 0.1751 | 0.2688 | 0.4977 | 0.4178 |
| $R$ | 0.4184 | 0.5185 | 0.7055 | 0.6464 |
| Case 2 | | | | |
| RMSE | 1.0709 | 0.2205 | 0.7616 | 0.1859 |
| Sd | 0.6699 | 0.1057 | 0.9875 | 0.1485 |
| $R^2$ | 0.3206 | 0.2169 | 0.6697 | 0.4350 |
| $R$ | 0.5662 | 0.4657 | 0.8183 | 0.6595 |
| Case 3 | | | | |
| RMSE | 1.0561 | 0.2296 | 0.5834 | 0.1550 |
| Sd | 0.8799 | 0.1480 | 1.1248 | 0.1930 |
| $R^2$ | 0.5531 | 0.4255 | 0.8689 | 0.7345 |
| $R$ | 0.7437 | 0.6523 | 0.9321 | 0.8570 |

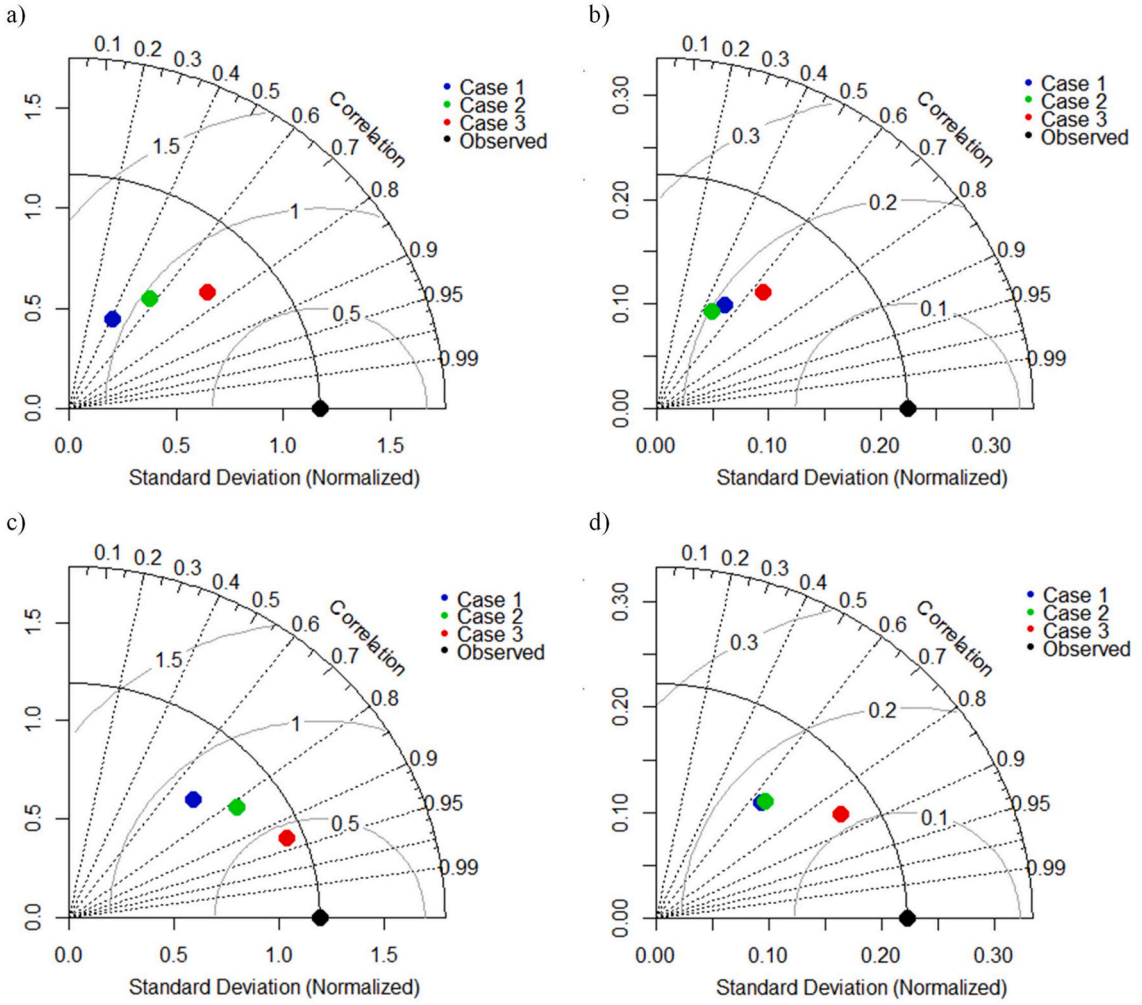


**Fig. 9.** Taylor diagram of the observed and predicted hydrobiological diversity indices of a) periphyton-H′, b) periphyton-J′, c) macrobenthos-H′, and d) macrobenthos-J'.

respectively (Fig. 9aandb); similar results for robust models were reported by Salih et al. [5] and Yaseen et al. [20]. The results of the model are related to the results of the PCA [21], and it is observed that factor F1 associated with the PPW data of case 1 does not correlate with the diversity indices. The F2 factor associated with the MCS data (As, Pb, and Zn) from case 2 correlated with the diversity indices of the macrobenthos but not with those of the periphyton. However, combining the PPW and MCS data improved model prediction.

The main advantage of the present predictive model lies in having rapid responses of the hydrobiological diversity of the basin function to the PPW and MCS, which can be used as early warnings for future changes in the composition of the basin's water. The limitation of the predictive model is the low amount of hydrobiological data of periphyton and macrobenthos necessary for a temporal prediction.

### 3.5. Multivariate analysis

PPW and MCS did not follow a normal distribution, and hydrobiological diversity indices followed a normal distribution according to the Jarque–Bera test. PCA, considering five factors, revealed a cumulative variability of 77.1% for PPW, MCS, and hydrobiological diversity data.

Factor F1 correlated with PPW, revealing that increased EC was linked to higher concentrations of bicarbonates (alkalinity), chlorides, sulfates, Ca, Mg, K, Na, and also corresponds to elevated temperatures during the dry season. Factor F2 was associated with the toxic influence of MCS, such As, Pb, and Zn, and the diversity and evenness of macrobenthos (Fig. 10). These heavy metals have a detrimental effect on aquatic insect macrobenthos because of their sedentary nature, because they spend several larval stages buried, and because they exhibit varied feeding habits. Multiple studies, including that by Mancilla-Villa et al. [49], have reported negative correlations between the concentrations of As, Pb, and Zn and the biotic indices of benthic communities. Factor F3 linked the geological Cu concentration and its impact as a nutrient on periphyton diversity and evenness. Research conducted by Balle et al. [50] suggests that Cu does not negatively affect the periphyton community and can potentially help to immobilize metals. Factor F4 is associated with Cr concentration and its role as a nutrient affect macrobenthos diversity. According to De Castro-Fernandez et al. [51], low metal concentrations, including those of Cr, appear to have a minimal impact on macrobenthos richness. Some macrobenthic species may have adapted to Cr levels. Finally, Factor F5 is linked to DO content, which may be associated with groundwater input, as indicated in Table 5.

No correlation was observed between DO and pH, which agrees with Fadel et al. [52], who suggested that there is either a weak or no connection between pH and DO in rivers. However, a previous study found a negative relationship between pH and DO in river systems [53]. This discrepancy may be due to the unique characteristics of the water sources and the impact of human activities on rivers. It is also important to mention that, except for the Capillune and Tumilaca stations, there was an inverse relationship between the temperature and DO levels. This observation agrees with similar findings in those of Zhong et al. [54] and Rajwa-Kuligiewicz et al. [55].

## 4. Conclusions

Developing a model for predicting diversity (H′) and evenness (J') indices for periphyton and macrobenthos based on information from PPW and MCS is essential for comprehensive monitoring of the basin and identifying possible changes caused by natural

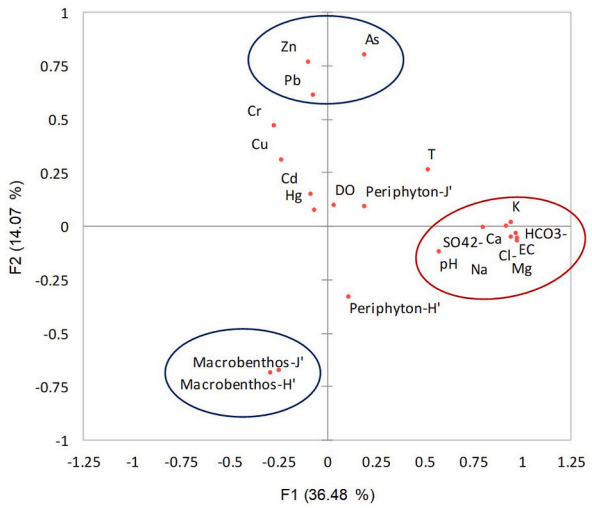


**Fig. 10.** PCA biplot of physicochemical composition of water (EC, DO, pH, T, $HCO_3^-$, $Cl^-$, $SO_4^{2-}$, Ca, Mg, K, Na), metal content in sediments (As, Hg, Cd, Cu, Cr, Pb, Zn), and hydrobiological diversity indices (periphyton-H′, periphyton-J′, macrobenthos-H′, macrobenthos-J′).

**Table 5**
Principal component analysis of physicochemical composition of water (EC, DO, pH, T, $HCO_3^-$, $Cl^-$, $SO_4^{2-}$, Ca, Mg, K, Na), metal content in sediments (As, Hg, Cd, Cu, Cr, Pb, Zn), and hydrobiological diversity indices (periphyton-H′, periphyton-J′, macrobenthos-H′, macrobenthos-J′).

| | F1 | F2 | F3 | F4 | F5 |
|---|---|---|---|---|---|
| As | 0.189 | **0.801** | −0.037 | −0.042 | 0.295 |
| Hg | −0.064 | 0.073 | −0.001 | 0.574 | −0.480 |
| Cd | −0.085 | 0.151 | −0.432 | −0.448 | −0.323 |
| Cu | −0.239 | 0.311 | **0.520** | 0.047 | 0.233 |
| Cr | −0.272 | 0.467 | 0.486 | −0.501 | −0.091 |
| Pb | −0.071 | **0.610** | 0.125 | −0.416 | 0.017 |
| Zn | −0.095 | **0.768** | 0.277 | −0.364 | −0.089 |
| Periphyton-H' | 0.108 | −0.331 | **0.773** | −0.193 | −0.336 |
| Periphyton-J' | 0.193 | 0.091 | **0.699** | 0.359 | −0.376 |
| Macrobenthos-H' | −0.292 | **−0.685** | 0.269 | −0.551 | −0.034 |
| Macrobenthos-J' | −0.250 | **−0.673** | 0.164 | −0.404 | 0.322 |
| EC | **0.976** | −0.056 | 0.096 | −0.056 | 0.010 |
| DO | 0.035 | 0.097 | 0.403 | 0.450 | 0.574 |
| pH | **0.571** | −0.122 | −0.147 | −0.302 | 0.153 |
| T | **0.514** | 0.264 | −0.485 | −0.110 | −0.165 |
| $HCO_3^-$ | **0.916** | −0.002 | −0.158 | −0.054 | 0.064 |
| $Cl^-$ | **0.944** | −0.049 | 0.132 | −0.038 | 0.000 |
| $SO_4^{2-}$ | **0.797** | −0.002 | 0.206 | 0.143 | 0.076 |
| Ca | **0.973** | −0.055 | 0.099 | −0.059 | 0.027 |
| Mg | **0.970** | −0.034 | 0.041 | −0.086 | −0.053 |
| K | **0.944** | 0.020 | 0.000 | −0.050 | −0.037 |
| Na | **0.972** | −0.066 | 0.111 | −0.068 | −0.004 |

processes associated with thaws or anthropogenic activities. Additionally, it provides information for developing preventative strategies and early warnings of possible future alterations. The results reveal that the MLRA model is efficient for predicting the H′ and J′ indices for macrobenthos when the model is based on the PPW and MCS. Furthermore, these results agree with the correlations obtained in the PCA.

When analyzing the major ions, the PPW did not impact periphyton or macrobenthos. Higher temperatures and increased EC in the Capillune River influenced the richness of macrobenthos, whereas temperature and intense radiation in the Tumilaca River promoted the richness of photosynthetic organisms while decreasing evenness. The presence of metals, such As, Pb, and Zn, in the sediments of the Asana-Tumilaca River Basin had a more significant effect on the diversity, evenness, and richness of macrobenthos. Conversely, the presence of other metals with nutritional properties, such as Cu and Cr, at low concentrations positively influenced the diversity of periphyton and macrobenthos species because of adaptive processes. Larger glacial melt areas during the 2019–2020 period altered the physicochemical parameters of the water, leading to increased metal concentrations in the sediment and habitat disturbances for organisms.

## Data availability statement

Data will be made available on request.

## Additional information

No additional information is available for this paper.

## Funding

The publication of this research was funded by German development cooperation, implemented by Deutsche Gesellschaft für Internationale Zusammenarbeit (GIZ) (GIZ) GmbH.

## CRediT authorship contribution statement

**Lisveth Flores del Pino:** Writing – review & editing, Supervision, Conceptualization. **Nancy Marisol Carrasco Apaza:** Writing – original draft, Investigation, Formal analysis, Data curation. **Víctor Caro Sánchez Benites:** Investigation, Formal analysis, Data curation. **Lena Asunción Téllez Monzón:** Formal analysis, Data curation. **Kimberly Karime Visitación Bustamante:** Investigation, Formal analysis, Data curation. **Jerry Arana-Maestre:** Investigation, Formal analysis, Data curation. **Diego Suárez Ramos:** Formal analysis, Data curation. **Ayling Wetzell Canales-Springett:** Writing – original draft, Formal analysis, Data curation. **Jacqueline Jannet Dioses Morales:** Writing – original draft, Formal analysis, Data curation. **Evilson Jaco Rivera:** Resources, Methodology. **Alex Uriarte Ortiz:** Resources, Methodology. **Paola Jorge-Montalvo:** Writing – review & editing, Software, Investigation, Formal analysis, Data curation. **Lizardo Visitación-Figueroa:** Writing – review & editing, Writing – original draft, Supervision, Formal analysis,

Conceptualization.

## Declaration of competing interest

The authors declare that they have no known competing financial interests or personal relationships that could have appeared to influence the work reported in this paper.

## Acknowledgements

The authors would like to thank the specialists from the Smithsonian Institution for their valuable contribution in supervision and mentoring this scientific article, to the German development cooperation, implemented by Deutsche Gesellschaft für Internationale Zusammenarbeit (GIZ) GmbH for its commitment to strengthening the capacities of Peru's Environmental Assessment and Enforcement Agency through the development of research.

## References

[1] M. Wang, B. De Vivo, S. Albanese, A. Lima, W. Lu, F. Molisso, M. Sacchi, Investigation on inorganic pollution level in surface sediments of Naples and Salerno Bay, Comput. Water, Energy, Environ. Eng. 2 (2013) 36–40, https://doi.org/10.4236/cweee.2013.22b006.
[2] M. Roncoroni, D. Mancini, F. Miesen, T. Müller, M. Gianini, B. Ouvry, M. Clémençon, F. Lardet, T.J. Battin, S.N. Lane, Decrypting the stream periphyton physical habitat of recently deglaciated floodplains, Sci. Total Environ. 867 (2023) 161374, https://doi.org/10.1016/j.scitotenv.2022.161374.
[3] Z. Gao, Z. Lin, F. Niu, J. Luo, M. Liu, G. Yin, Hydrochemistry and controlling mechanism of lakes in permafrost regions along the Qinghai-Tibet Engineering Corridor, China, Geomorphology 297 (2017) 159–169, https://doi.org/10.1016/j.geomorph.2017.09.020.
[4] Y.E. Joelle, T. Emile, K. Lucas, A. Jean-Paul, M.N. Mathieu, S.T.F. Brice, W.F. Robean, T.K. Brice, Hydro-geochemistry of groundwater and surface water in Dschang town (West Cameroon): alkali and alkaline-earth elements ascertain lithological and anthropogenic constraints, J. Groundw. Sci. Eng. 9 (2021) 212–224, https://doi.org/10.19637/j.cnki.2305-7068.2021.03.004.
[5] S.Q. Salih, I. Alakili, U. Beyaztas, S. Shahid, Z.M. Yaseen, Prediction of dissolved oxygen, biochemical oxygen demand, and chemical oxygen demand using hydrometeorological variables: case study of Selangor River, Malaysia, Environ. Dev. Sustain. 23 (2021) 8027–8046, https://doi.org/10.1007/s10668-020-00927-3.
[6] V. Pandey, B. Chotaliya, N. Bist, K. Yadav, A. Sircar, Geochemical analysis and quality assessment of geothermal water in Gujarat, India, Energy Geosci 4 (2023) 59–73, https://doi.org/10.1016/j.engeos.2022.08.001.
[7] N. Kumar Ravi, P. Kumar Jha, K. Varma, P. Tripathi, S. Kumar Gautam, K. Ram, M. Kumar, V. Tripathi, Application of water quality index (WQI) and statistical techniques to assess water quality for drinking, irrigation, and industrial purposes of the Ghaghara River, India, Total Environ. Res. Themes 6 (2023) 100049, https://doi.org/10.1016/j.totert.2023.100049.
[8] K. Visitación, L. Ramos, L. Visitación, Caracterización hidroquímica de una subcuenca altoandina en el departamento de Moquegua, Perú, Tecnol. y Ciencias Del Agua 0 (2022) 1–34, https://doi.org/10.24850/j-tyca-14-5-6.
[9] M.K. Kadim, Y. Risjani, Biomarker for monitoring heavy metal pollution in aquatic environment: an overview toward molecular perspectives, Emerg. Contam. 8 (2022) 195–205, https://doi.org/10.1016/j.emcon.2022.02.003.
[10] M. Nowrouzi, A. Pourkhabbaz, Application of geoaccumulation index and enrichment factor for assessing metal contamination in the sediments of Hara Biosphere Reserve, Iran, Chem. Speciat. Bioavailab. 26 (2014) 99–105, https://doi.org/10.3184/095422914X13951584546986.
[11] C.A. Vasquez, N. León-Roque, J.L. Nuñez-León, D.W. Hidalgo-Chávez, J. Oblitas, Geochemical and environmental assessment of potential effects of trace elements in soils, water, and sediments around abandoned mining sites in the northern Iberian Peninsula (NW Spain), Heliyon 9 (2023) e14659, https://doi.org/10.1016/j.heliyon.2023.e14659.
[12] Y. Ban, T. Lei, C. Chen, Z. Liu, Study on the facilities and procedures for meltwater erosion of thawed soil, Int. Soil Water Conserv. Res. 4 (2016) 142–147, https://doi.org/10.1016/j.iswcr.2016.04.003.
[13] C. Poussin, P. Timoner, B. Chatenoux, G. Giuliani, P. Peduzzi, Improved Landsat-based snow cover mapping accuracy using a spatiotemporal NDSI and generalized linear mixed model, Sci. Remote Sens. 7 (2023) 100078, https://doi.org/10.1016/j.srs.2023.100078.
[14] B. Ochieng, E.O. Mbao, Z. Zhang, L. Shi, Q. Liu, Phytoplankton community structure of Tang-Pu Reservoir: status and ecological assessment in relation to physicochemical variability, Environ. Monit. Assess. 194 (2022) 1–14, https://doi.org/10.1007/s10661-022-09958-x.
[15] C. Veloy, M. Hidalgo, M.G. Pennino, E. Garcia, A. Esteban, C. García-Ruiz, G. Certain, S. Vaz, A. Jadaud, M. Coll, Spatial-temporal variation of the Western Mediterranean Sea biodiversity along a latitudinal gradient, Ecol. Indic. 136 (2022) 108674, https://doi.org/10.1016/j.ecolind.2022.108674.
[16] T. Salvatierra-Suárez, Macroinvertebrados acuáticos como indicadores biológicos de la calidad del agua en el río Gil González y tributarios más importantes, Rivas, Nicaragua, Rev. Univ. y Cienc. 6 (2012) 38–46, https://doi.org/10.5377/uyc.v6i9.1958.
[17] I. Katano, J.N. Negishi, T. Minagawa, H. Doi, Y. Kawaguchi, Y. Kayaba, Effects of sediment replenishment on riverbed environments and macroinvertebrate assemblages downstream of a dam, Sci. Rep. 11 (2021) 1–17, https://doi.org/10.1038/s41598-021-86278-z.
[18] D.S.N. Munasinghe, M.M.M. Najim, S. Quadroni, M.M. Musthafa, Impacts of streamflow alteration on benthic macroinvertebrates by mini-hydro diversion in Sri Lanka, Sci. Rep. 11 (2021) 1–12, https://doi.org/10.1038/s41598-020-79576-5.
[19] C.H. Hay, T.G. Franti, D.B. Marx, E.J. Peters, L.W. Hesse, Macroinvertebrate drift density in relation to abiotic factors in the Missouri River, Hydrobiologia 598 (2008) 175–189, https://doi.org/10.1007/s10750-007-9149-3.
[20] Z.M. Yaseen, M. Ali, A. Sharafati, N. Al-Ansari, S. Shahid, Forecasting standardized precipitation index using data intelligence models: regional investigation of Bangladesh, Sci. Rep. 11 (2021) 1–25, https://doi.org/10.1038/s41598-021-82977-9.
[21] A.K. Panja, S. Vasavdutta, M. Choudhary, I. Thiyagarajan, A.H. Shinde, S. Ray, T.P. Sahoo, S. Chatterjee, R.B. Thorat, A.K. Madhava, S. Haldar, Interaction of physico-chemical parameters with Shannon-Weaver Diversity Index based on phytoplankton diversity in coastal water of Diu, India, Mar. Pollut. Bull. 190 (2023) 114839, https://doi.org/10.1016/j.marpolbul.2023.114839.
[22] H. Jeong, S. Park, B. Choi, C.S. Yu, J.Y. Hong, T.Y. Jeong, K.H. Cho, Machine learning-based water quality prediction using octennial in-situ Daphnia magna biological early warning system data, J. Hazard Mater. 465 (2024) 133196, https://doi.org/10.1016/j.jhazmat.2023.133196.
[23] D.B. Montesinos, A.M. Cleef, K.V. Sýkora, Andean shrublands of Moquegua, south Peru: prepuna plant communities, Phytocoenologia 42 (2012) 29–55, https://doi.org/10.1127/0340-269X/2012/0042-0516.
[24] M.S. Bin Aziz, N.A. Hasan, M.M.R. Mondol, M.M. Alam, M.M. Haque, Decline in fish species diversity due to climatic and anthropogenic factors in Hakaluki Haor, an ecologically critical wetland in northeast Bangladesh, Heliyon 7 (2021) e05861, https://doi.org/10.1016/j.heliyon.2020.e05861.
[25] S. Nuraeni, M. Rajab, Tumanan, D. Wahyudi, Identification of insects associated with ebony (Diospyros celebica Bakh.) as an endemic tree to Sulawesi, IOP Conf. Ser. Earth Environ. Sci. 886 (2021) 012037, https://doi.org/10.1088/1755-1315/886/1/012037.
[26] M. Tripathi, S.K. Singal, Use of principal component analysis for parameter selection for development of a novel water quality index: a case study of river ganga India, Ecol. Indic. 96 (2019) 430–436, https://doi.org/10.1016/j.ecolind.2018.09.025.
[27] R. Coccioni, F. Frontalini, A. Marsili, D. Mana, Benthic foraminifera and trace element distribution: a case-study from the heavily polluted lagoon of Venice (Italy), Mar. Pollut. Bull. 59 (2009) 257–267, https://doi.org/10.1016/j.marpolbul.2009.08.009.

[28] S. Muyasaroh, B.S. Muntalif, Determination of surface water quality based on macrozoobenthos biodiversity and the prevalence of trematodes cercariae in freshwater molluscs, Malaysian Appl. Biol. 49 (2020) 19–25, https://doi.org/10.55230/mabjournal.v49i2.1518.
[29] J. Jiang, S. Tang, D. Han, G. Fu, D. Solomatine, Y. Zheng, A comprehensive review on the design and optimization of surface water quality monitoring networks, Environ. Model. Softw. 132 (2020) 104792, https://doi.org/10.1016/j.envsoft.2020.104792.
[30] T. Tsering, M.S.M. Abdel Wahed, S. Iftekhar, M. Sillanpää, Major ion chemistry of the Teesta River in Sikkim Himalaya, India: chemical weathering and assessment of water quality, J. Hydrol. Reg. Stud. 24 (2019) 100612, https://doi.org/10.1016/j.ejrh.2019.100612.
[31] R.P. Reid, A.M. Oehlert, E.P. Suosaari, C. Demergasso, G. Chong, L.V. Escudero, A.M. Piggot, I. Lascu, A.T. Palma, Electrical conductivity as a driver of biological and geological spatial heterogeneity in the Puquios, Salar de Llamara, Atacama Desert, Chile, Sci. Rep. 11 (2021) 12769, https://doi.org/10.1038/s41598-021-92105-2.
[32] K.E. Relph, E.I. Stevenson, A.V. Turchyn, G. Antler, M.J. Bickle, J.J. Baronas, S.E. Darby, D.R. Parsons, E.T. Tipper, Partitioning riverine sulfate sources using oxygen and sulfur isotopes: implications for carbon budgets of large rivers, Earth Planet Sci. Lett. 567 (2021) 116957, https://doi.org/10.1016/j.epsl.2021.116957.
[33] T.A. Carrino, A.P. Crósta, C.L.B. Toledo, A.M. Silva, J.L. Silva, Geology and hydrothermal alteration of the Chapi Chiara prospect and nearby targets, Southern Peru, using ASTER data and reflectance spectroscopy, Econ. Geol. 110 (2015) 73–90, https://doi.org/10.2113/econgeo.110.1.73.
[34] S.R. Taylor, Abundance of chemical elements in the continental crust : a new table, Geochim. Cosmochim. Acta 28 (1964) 1273–1285, https://doi.org/10.1016/0016-7037(64)90129-2.
[35] S. Villacorta, L. Fidel, B. Zavala, Mapa de susceptibilidad por movimientos en masa del Perú, Rev. La Asoc. Geológica Argentina 69 (2012) 393–399. https://revista.geologica.org.ar/raga/article/view/524.
[36] P. Böning, H.J. Brumsack, M.E. Böttcher, B. Schnetger, C. Kriete, J. Kallmeyer, S.L. Borchers, Geochemistry of Peruvian near-surface sediments, Geochim. Cosmochim. Acta 68 (2004) 4429–4451, https://doi.org/10.1016/j.gca.2004.04.027.
[37] M. Balali-Mood, K. Naseri, Z. Tahergorabi, M.R. Khazdair, M. Sadeghi, Toxic mechanisms of five heavy metals: mercury, lead, chromium, cadmium, and arsenic, Front. Pharmacol. 12 (2021) 1–19, https://doi.org/10.3389/fphar.2021.643972.
[38] S. Nazneen, S. Jayakumar, M.F. Albeshr, S. Mahboob, I. Manzoor, J. Pandiyan, K. Krishnappa, M. Rajeswary, M. Govindarajan, Analysis of toxic heavy metals in the pellets of owls: a novel approach for the evaluation of environmental pollutants, Toxics 10 (2022) 693, https://doi.org/10.3390/toxics10110693.
[39] R.D. Díaz Aguilar, S.V. Sanchez Larico, E. Lujano Laura, A. Lujano Laura, Análisis multi-temporal entre 1975 y 2015 sobre cambios de la cobertura glaciar en los nevados Allin Capac y Chichi Capac, Perú, Rev. Investig. Altoandinas 19 (2017) 265–274, https://doi.org/10.18271/ria.2017.291.
[40] F.S. Monge-Rodríguez, C. Huggel, L. Vicuna, Perception of glacial retreat and climate change in Peruvian Andean communities: an interdisciplinary approach, Ambient. e Soc. 25 (2022), https://doi.org/10.1590/1809-4422ASOC20200227R2VU2022L3AO.
[41] H. Montoya T, J.A. Fiestas I, R. Cruz S, R. Quispe P, S. Rodríguez V, Comunidades criofílicas de los glaciares del nevado de Allincapac, Andes del sur de Perú, departamento de Puno: variabilidad fenotípica de la cianobacteria Nostoc commune (Nostocales, Nostocaceae), Arnaldoa 26 (2019) 657–674, https://doi.org/10.22497/arnaldoa.261.26209.
[42] C. Villamarín, N. Prat, M. Rieradevall, Caracterización física, química e hidromorfológica de los ríos altoandinos tropicales de Ecuador y Perú, Lat. Am. J. Aquat. Res. 42 (2014) 1072–1086, https://doi.org/10.3856/vol42-issue5-fulltext-12.
[43] J. Arana, C. Cabrera, Macroinvertebrados acuáticos y caracterización ecológica de los ambientes dulceacuícolas del área de influencia del gasoducto PERÚ LNG en los departamentos de Ica y Huancavelica, Rev. Del Inst. Investig. La Fac. Minas, Metal, y Ciencias Geográficas 20 (2017) 86–93, https://doi.org/10.15381/iigeo.v20i40.14394.
[44] M.P. Venarsky, V. Lowe, C.L.J. Frid, M.A. Burford, Flow regimes among rivers influences benthic biota biodiversity, but not abundance or biomass, in intertidal mudflats and sandflats in wet-dry tropical estuaries, Estuar. Coast Shelf Sci. 271 (2022) 107858, https://doi.org/10.1016/j.ecss.2022.107858.
[45] Z. Huang, R. Bi, S. Musil, Á.H. Pétursdóttir, B. Luo, P. Zhao, X. Tan, Y. Jia, Arsenic species and their health risks in edible seaweeds collected along the Chinese coastline, Sci. Total Environ. 847 (2022) 157429, https://doi.org/10.1016/J.SCITOTENV.2022.157429.
[46] Q. Zhao, P.J. Van den Brink, C. Xu, S. Wang, A.T. Clark, C. Karakoç, G. Sugihara, C.E. Widdicombe, A. Atkinson, S.S. Matsuzaki, R. Shinohara, S. He, Y.X. G. Wang, F. De Laender, Relationships of temperature and biodiversity with stability of natural aquatic food webs, Nat. Commun. 14 (2023), https://doi.org/10.1038/s41467-023-38977-6.
[47] C. Carrasco, C. Rayme, R.D.P. Alarcón, Y. Ayala, J. Arana, H. Aponte, Aquatic macroinvertebrates in streams associated with high andean wetlands of Ayacucho Peru, Rev. Biol. Trop. 68 (2020), https://doi.org/10.15517/rbt.v68is2.44344. S116–S131.
[48] J. Alomía, J.A. Iannacone, L. Alvariño, K. Ventura, Macroinvertebrados bentónicos para evaluar la calidad de las aguas de la cuenca alta del río Huallaga, Perú, Biol. 1 (2017) 65–84, https://doi.org/10.24039/rtb2017151144.
[49] O.R. Mancilla-Villa, L. Gómez-Villaseñor, C. Palomera-García, O. Hernández-Vargas, R.D. Guevara-Gutiérrez, H.M. Ortega-Escobar, H. Flores-Magdaleno, Á. Can-Chulim, E.I. Sánchez-Bernal, J.U. Avelar-Roblero, E. Cruz-Crespo, Heavy metals in water and macroinvertebrates of the Ayuquila-Armería river basin (Mexico) and its affluents, Terra Latinoam 41 (2023) 1–17, https://doi.org/10.28940/terra.v41i0.1603.
[50] M.G. Balle, C. Ferragut, L.H.G. Coelho, T.A. de Jesus, Phosphorus and metals immobilization by periphyton in a shallow eutrophic reservoir, Acta Limnol. Bras. 33 (2021) e11, https://doi.org/10.1590/S2179-975X0320.
[51] P. De Castro-Fernández, L. Cardona, C. Avila, Distribution of trace elements in benthic infralittoral organisms from the western Antarctic Peninsula reveals no latitudinal gradient of pollution, Sci. Rep. 11 (2021) 16266, https://doi.org/10.1038/s41598-021-95681-5.
[52] A. Fadel, M. Kanj, K. Slim, Water quality index variations in a Mediterranean reservoir: a multivariate statistical analysis relating it to different variables over 8 years, Environ. Earth Sci. 80 (2021) 1–13, https://doi.org/10.1007/s12665-020-09364-x.
[53] H. Wu, C. Jiang, Z. Du, Long-term trends of water quality in upstream of daling river in China, Adv. Mater. Res. 599 (2012) 673–677, https://doi.org/10.4028/www.scientific.net/AMR.599.673.
[54] M. Zhong, S. Liu, K. Li, H. Jiang, T. Jiang, G. Tang, Modeling spatial patterns of dissolved oxygen and the impact mechanisms in a cascade river, Front. Environ. Sci. 9 (2021) 1–10, https://doi.org/10.3389/fenvs.2021.781646.
[55] A. Rajwa-Kuligiewicz, R.J. Bialik, P.M. Rowiński, Dissolved oxygen and water temperature dynamics in lowland rivers over various timescales, J. Hydrol. Hydromechanics 63 (2015) 353–363, https://doi.org/10.1515/johh-2015-0041.